Modelling Perth Photochemical Smog Events Using the Urban Airshed Model

Dr Peter Rye

Contents

1. Introduction

In 1989 the W.A. Department of Environmental Protection established an air quality monitoring station Caversham (See Figure 1). The purpose of this station was to measure concentrations of ozone and nitrogen oxides downwind of the city, in conditions with potential to generate photochemical smog.

Measured hourly averages of ozone in excess of 80 ppb (Canadian / W.H.O. acceptable limit) indicated that Perth was experiencing at least the beginnings of photochemical smog. The Perth Photochemical Smog Study was subsequently undertaken by Western Power and the Department of Environmental Protection, to provide a detailed understanding of the occurrence of smog events, over the whole of the Perth region.
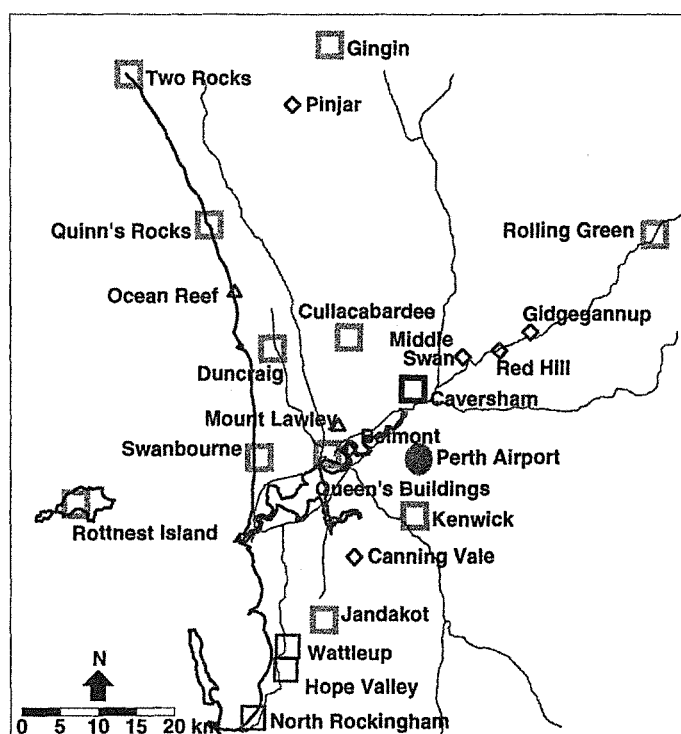
Figure 1. Measurement sites used in the Perth Photochemical Smog Study. See sections 1 and 3 for explanation of sites.

The major components of the study included the continuous monitoring of photochemical smog species (at the Caversham site, and shaded sites in Figure 1) and of meteorological variables, the development of an emissions inventory, and adaptation of existing computer models to represent the transport and photochemistry of smog in the region. In addition, a major field measurement exercise was conducted through the summer of 1993-1994, with the aim of characterising in detail a number of photochemical smog events.

The modelling component of the study was to include contributions from consultants and from within the Department of Environmental Protection. The latter included both meteorological modelling, using the author's own three-dimensional model, reported separately (Rye, 1996b), and photochemistry modelling using the Urban Airshed Model.

2. Overview of Perth's Photochemical Smog Events

The Perth metropolitan area experiences about ten events each year when the concentration of ozone within photochemical smog exceeds 80 ppb. Over the period 1989-1995, when measurements have been available from Caversham (See Figure 1), there has been no detectable trend in this frequency. The highest events, occurring once every year or two, have peak concentrations in the vicinity of 120 ppb.

Smog events occur in association with sea breezes, peak ozone concentrations occurring just after their arrival. Initial analyses showed that highest concentrations occur to the north east of the city when a morning north easterly wind carries urban emissions offshore, and a south westerly sea breeze develops and brings the reacting air mass back over the city.

For morning winds to be from the north east, a low pressure trough is generally located offshore. Winds near the trough axis tend to be light, and relatively cool temperatures on the offshore side of the trough appear to contribute to high smog concentrations, by reducing mixing depths when the surface south westerly brings the air inland. This means that, in general, Perth's highest smog concentrations occur in association with the passage inland of a weak low pressure trough.

An analysis of smog events through the three years of the Perth Photochemical Smog Study (Rye, 1996b) showed that few involved return of other than the emissions generated on the day of the event. This meant that most model studies required no more than one day's simulation. In some cases - particularly when the parametric sensitivity of an afternoon ozone peak was at issue - less than a full day's simulation gave useful results.

3. Outline of the Urban Airshed Model

This model (subsequently termed "UAM") was written originally for the U.S. EPA during 1969-1973, under contract by Systems Applications Inc. Its history has been well documented by Scheffe and Morris (1993).

3.1. Model Structure

UAM performs calculations on a three-dimensional grid. The west-east and south-north horizontal grid intervals are uniform, typically 3 km each. In the vertical, the grid is defined relative to the ground surface, mixing depth and the top of the modelled region. Grid intervals are uniform from the ground to the mixing depth (termed "diffusion break" in the model's documentation), and from the mixing depth to the top of the modelled region. Typically, there are three layers below and above the mixing depth (Figure 2).

The model represents essentially four groups of processes - emissions, transport, chemical transformation and deposition.

Emissions of chemical components can occur at any point in the grid. Surface-based emissions, such as from vehicles, are included in layer 1 of the model. Elevated emissions (such as from tall chimney stacks) are added in the model layer which includes their final level, after completion of plume rise.

The advection (transport) of smog components is performed using a three-dimensional wind field for each layer of the model. Advection schemes normally represent a compromise between avoidance of spurious numerical diffusion, and the occurrence of small negative concentrations at plume boundaries. When chemical reaction rates are calculated, these
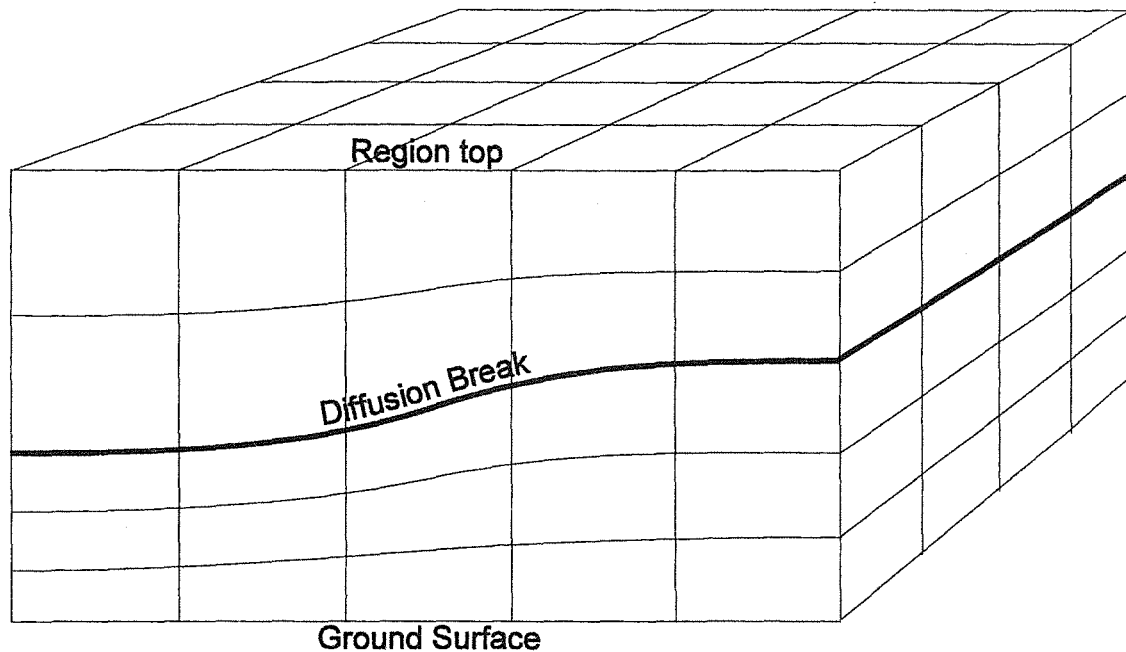
Figure 2. Illustration of the grid stucture used by the Urban Airshed Model. The case here comprises a grid with 5 cells left-to-right, 4 cells front-to-back, 3 layers below the diffusion break, and two layers above. A left-to-right variation of the height of the diffusion break is shown, altering layer thicknesses across the grid.

negative concentrations can cause significant modelling errors. UAM incorporates an advection scheme which maintains positive concentration estimates, while minimising numerical diffusion.

The formation of photochemical smog involves numerous individual chemical reactions, which can not be completely represented on the basis of current knowledge and within the limitations of present computers. As a result, chemical transformations are modelled using a simplified version of the reaction set. The mechanism used in UAM is known as Carbon Bond IV, which groups reactions according to the structure of the carbon bonds of the reacting species. Nevertheless, the set remains complex, involving 24 species and 94 separate reactions. Details of this scheme are provided by Morris and Myers (1990, their chapter 2.3 and Appendix A).

Second only to transport out of the grid, deposition of smog products is the next most important means of their removal from the modelled region. UAM includes a classification of surface types based on land use, and deposition calculations use the vegetation and surface roughness combinations implict in each surface type. The scheme used in UAM is described in detail by Killus et al. (1984)

The sole modifications made, in this study, to the code of the model were to write the current model time to a file, at each model timestep (for reliable tracing of model progress), and writing of two forms of output of the "instant" concentrations. The latter was added to allow better tracing of the time sequence of concentrations when sharp, short peaks passed a site, without generating too large a set of output files. It involved output of the full three-dimensional concentration set at hourly intervals, and of the concentrations in model layer 1 at 10-minute intervals.

3

3.2. Data Requirements

Required input emissions species comprised nitric oxide, nitrogen dioxide, carbon monoxide, paraffins, ethylene, olefins, isoprene, toluene, xylene, formaldehyde and higher aldehydes. Of these, the organics (commencing with paraffins) are largely surrogates for a range of chemical species (Morris and Myers, 1990). Area-based, vehicular, surface industrial and biogenic emissions were provided as one data set, on a horizontal grid matching the UAM computational grid. Emissions from elevated industrial sources were catalogued by location, the mix of emissions, stack height, diameter, volume flow and emission temperature. These were provided in a separate file, the calculation of horizontal grid location and insertion level being performed within UAM.

A detailed summary of emissions used is provided in section 4 of this report.

The meteorological data required by the model comprises horizontal winds at all model levels, mixing depths, surface temperatures, solar radiation, and representative stability estimates above and below the mixing depth. The vertical wind velocity is calculated internally, to ensure that a nondivergent state consistent with its own advection scheme is maintained.

Either measured or modelled meteorological fields could be used, with site measurements being interpolated to three- or two-dimensional grids in the former case. When measurements were input to the model, measured solar radiation was used, and calculated clear-sky radiation was used when modelled meteorology was selected. Due to mixing depth changes across the region, the required stability estimates were not spatially constant, so a representative location was used. The values used were those calculated for a location initially on the central business district, following the motion of the air mass after 8 a.m..

Sources of meteorological data are described in sections 5 and 6.

Boundary and initial conditions for ozone and nitrogen oxides were defined using measurements at monitoring sites receiving air from rural regions - usually, Rolling Green or Two Rocks (See Figure 1). Nonzero initial and boundary values for the paraffin surrogate (14 ppb) and formaldehyde (2 ppb) were also used, the former being a default value provided with the model files, the latter being an estimate of the product from the previous day's biogenic isoprene emissions.

The model also required land use classifications, for definition of surface transfer coefficients. These were provided as a component of the area-based emissions inventory (Stuart and Carnovale, 1994).

4. Emissions Inventory

The estimates of emissions of smog precursors were provided by four sources, as inventories of vehicle, industrial, area and biogenic emissions.

4.1. Vehicle Emissions

These were estimated by the Western Australian Department of Transport (James, 1995), using road usage information provided by the Western Australian Main Roads Department, the state's register of motor vehicles, and emissions factors determined by the Environmental Protection Authorities of Victoria and New South Wales. Total vehicles kilometres travelled ("VKT"), classified according to vehicle type, age and mode of travel, were analysed as a

function of time of day. The emissions factors were used to convert the classified VKT to emissions estimates.

Resulting emissions estimates, for carbon monoxide, ROC, nitrogen oxides, sulphur dioxide, lead and particulates, were summed to give gridded emissions totals. Projections to later years were also made, based on altered population distributions, vehicle mix and aging of catalytic converters. A detailed analysis was provided by James (1995).

Estimates were tabulated for 1986 and 1991, with trend estimates, as percentages of 1986 emissions for carbon monoxide, hydrocarbons and nitrogen oxides, extending to 2011. The trend estimates were used to produce inventories appropriate for any required year.

4.2. Area Sources

The area source inventory was based on a range of emissions factors drawn from Victorian experience, and supplementary local information (Stuart and Carnovale, 1994). Separate estimates were made for emissions from surface coatings, service station activities, domestic and commercial aerosols, natural gas leakage, bitumen surfacing, lawn mowing, dry cleaning, domestic natural gas combustion, domestic solid and liquid fuel combustion, solvents, domestic waste combustion, and miscellaneous sources such as railways, marine craft and off-road vehicles.

Final emissions estimates were calculated using these emissions factors and gridded population estimates, for which 1992 and 2002 distributions were provided. For other years, a linear interpolation was used to calculate the gridded populations required.

4.3. Industrial Sources

Industrial emissions were catalogued using reponses to questionnaires, and from electricity and gas use information provided by Western Power. In all, 77 elevated sources, 105 surface sources and 41 sources of fugitive reactive organic carbon compounds ("ROC") were recorded.

Industrial emissions were based generally on the year 1992, with some applicable to 1991, and some to the 1992-1993 financial year. The estimates used for any year's emissions were taken to be proportional to total population, without any general expansion of the source distribution.

Comparisons of inventory estimates and measured fluxes, made using aircraft observations during the intensive study period of PPSS, showed some discrepancies. Measurements indicated hydrocarbon fluxes from the Kwinana industrial area were about 1.2 kg s^{-1} (Carras, Clark, Hacker, Nelson and Williams, 1995), while inventory estimates totalled 0.5 kg s^{-1}. There were also indications from bag samples that significant differences occurred in the species emitted. Early analyses of the reactivity of plumes indicated a greater difference, by factors of up to four. Although this factor was later revised downward (Berko, personal communication), an adjustment factor of three was normally used for Kwinana ROC emissions.

4.4. Biogenic Emissions

Previous studies (e.g., Carnovale et al. 1991) have found that biogenic emissions can amount to over 10% of the total volatile organic carbon emissions for a region. Moreover, the compounds emitted, principally isoprene and a group termed monoterpenes, are highly reactive.

5

Biogenic emissions are by nature "fugitive", not being emitted as a consequence of any specific process. Estimates were therefore based on emissions factors for a range of vegetation types occurring in the region. Development of this part of the inventory required knowledge of the distribution of natural vegetation types, and the fractional cover of each type.

The dominant vegetation cover in 3km grid squares across the Perth region was found from published vegetation maps (Beard, 1979a, 1979b - see Figure 3). The fractional cover of natural vegetation was also estimated, using Landsat photographs of the region (Weir, personal communication).

Legend:
- Jarrah/marri forest
- Open marri woodland
- Jarrah/marri/sheoak/banksia
- Tuart woodland
- Banksia/sheoak woodland
- Banksia low woodland
- Swampy, sheoak/melaleuca
- Coastal heath
- Pine plantation
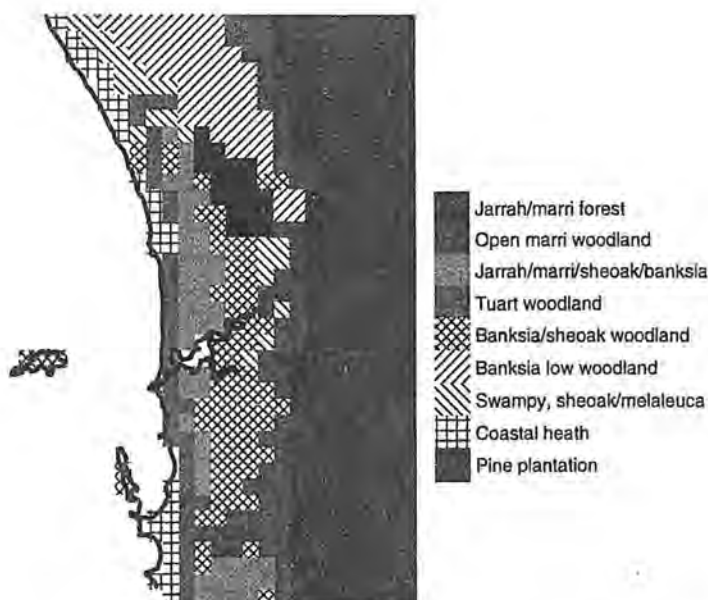
*Figure 3. Natural vegetation of the Perth region (after Beard, 1979a, 1979b)*

From these records, measured canopy densities (Hingston, Dimmock and Turton, 1980) and published canopy emissions rates (Guenther, Zimmerman and Wildermuth, 1994; Lamb, Gay and Westberg, 1993), emissions of monoterpenes and isoprene could be found. Tests showed that, in order to generate emissions consistent with measurements, the factors published by Lamb et al. were required, with branch-level rather than leaf-level emissions factors.

A simple parameterisation of biogenic emissions of nitrogen oxides was also included. Ten categories matched to land use (urban, agricultural, rangeland, deciduous forest, coniferous forest, mixed forest, water, other, wetland, mixed agricultural and rangeland) were defined, with emissions factors supplied by Cope (personal communication). The level of emissions which resulted was only a minor fraction of the NO_x overall emissions inventory, and had no discernible effect on calculated concentrations.

4.5. General Pattern of Emissions

Figure 4 shows a summary of the pattern of emissions estimates for 1994, for the emitted nitrogen oxides. Surface emissions follow closely the distribution of population, with the exception of emissions from the Kwinana industrial area, and a low general background from rural land. The only elevated sources of sufficient size to show in the figure are the Kwinana

and Canning Vale industrial areas, takeoff and landing paths for airports, the Pinjar power station and a small number of other isolated industries.
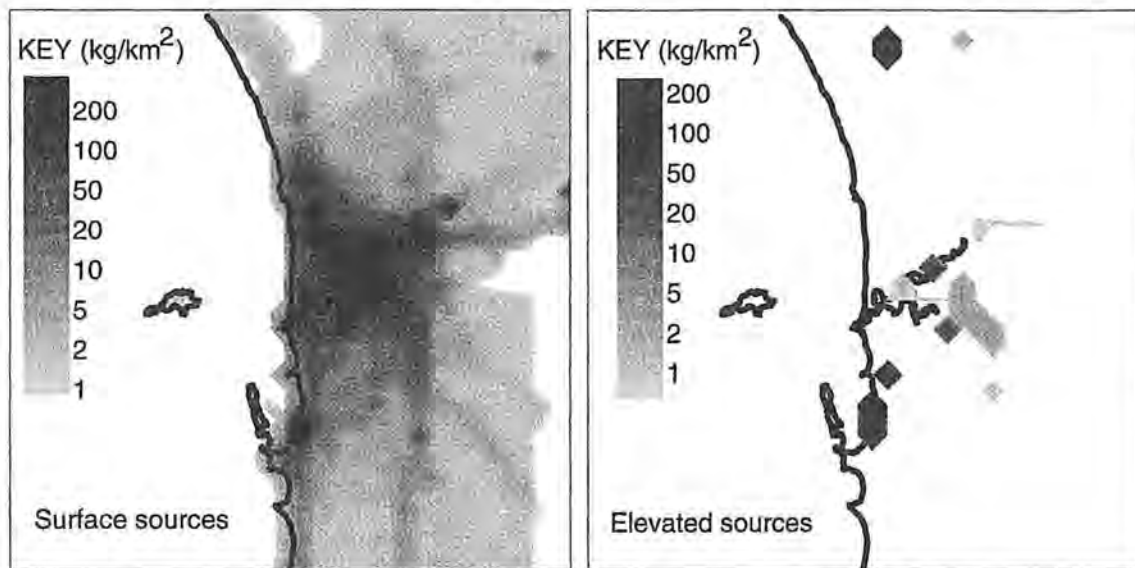
Figure 4. Total daily emissions of nitrogen oxides (expressed as equivalent nitric oxide) for a 1994 Perth weekday, combining all emissions sources, in kg/km². The peak emission rate for elevated sources was 2580 kg/km².

5. Modelled Meteorological Data

In coastal regions of Australia, the effects of sea breezes and topography often mean that winds, mixing depths and temperatures change considerably over a short distance. Measuring these changes routinely over the whole region, at a sufficient resolution, would have required more measurement sites than economically possible.

The normal approach taken in these circumstances is to model the meteorology of the region at high resolution, using a three-dimensional primitive equation model. Both the initialisation and validation data used by such models are provided by a surface and upper-level measurement programme. When model calculations agree closely with the available measurements, the modelled fields can be used as input to UAM.

Any such meteorological model may be used to provide input data, the model used for the work reported here being the author's own (Rye, 1989, 1996b). This did not include the effects of topography, but possessed the marked advantages of rapid execution, and ability to use a nonuniform initialisation. The former meant that higher resolution and more detailed validation were possible, while the latter ensured that the effects of the coastal trough could be incorporated.

In order to represent the meteorology of a trough day, it was necessary to generate firstly a fair representation of the coastal trough. Spatial data for this task were not readily available, so the trough was generated by running the model for an extended period, from a reasonable starting condition. The initial model runs used a west-east resolution of 12 km, and a north-south resolution of 40 or 80 km. With a grid size of 120 x 30 or 120 x 15, the modelled region covered most of the southern part of Western Australia, extending about 750 km to the west of Perth.

It was found that, in many cases, the trough would develop from a horizontally uniform wind field, with thermal-wind-derived temperature gradients. The data used were a morning temperature sounding obtained at Perth Airport, augmented by higher-resolution wind and temperature measurements obtain using a sodar and RASS radar at Cullacabardee (See Figure 1). However, insertion of an initial approximation to the surface pressure field always assisted the formation of the trough, and sometimes was essential for it to occur at all.

A detailed description of the modelling process, and comparison of modelled and measured fields, is given by Rye (1996b).

Once a successful regional representation of the trough was achieved, the model was re-run at high resolution (6 x 10 km, or 3 x 5 km, west-east and north-south), nested within the fields calculated in the first model run. Three-dimensional wind, mixing depth and temperature fields were written at half-hourly intervals, and these were later processed to generate input files used by UAM.

6. Measured Meteorological Data

For some days, sufficient monitoring data were available to permit creation of input fields by interpolation. This process was assisted by observations, in measurement and modelling, that most variations occurred in a direction perpendicular to the coastline.

The analysis software provided with UAM was found to be unsuitable for the task of converting point measurements to input fields. Because it included a sophisticated divergence mimisation scheme, it generated windfields from which the sea breeze was heavily filtered. The sea breeze was known to be central to the development of photochemical smog in the region, so use of this component of the UAM software set was discontinued in favour of a tailored module of the locally-written preprocessor program.

Two interpolation schemes were included in this data preparation program. One was a simple inverse-squares weighting scheme, and the other was an implementation of the scheme described by Goodin, McRae and Seinfeld (1979). The latter used a detailed triangulation of the study region, but, with a variable number of operational sites, it was necessary to recalculate the optimum triangulation at each time step. Although this scheme provided slightly superior field interpolations, the time required proved prohibitive, so it was not generally used.

The data interpolation included a longshore bias, reflecting the observed windfield structure. Typically, when using inverse-squares weighting factors, distances were separated into alongshore and onshore components. (Based on the measured wind velocity cross-correlation pattern, a direction of 174° was taken to correspond to longshore) Before calculating the "radius" to each measurement point, the onshore component was multiplied by three.

The full set of measurement points used was as follows (See Figure 1 for locations):

Surface measurements: Rottnest Island, Two Rocks, Quinn's Rocks, Ocean Reef, Swanbourne, Jandakot, Wattleup, Hope Valley, Canning Vale, Belmont, Cullacabardee, Pinjar, Caversham, Kenwick, Middle Swan, Gidgegannup, Rolling Green. (Also, for the 1994-1995 summer, Gingin, Duncraig and Mount Lawley)

Vertical profile measurements: Rottnest Island, Swanbourne, Rolling Green (1995) Gidgegannup (to 1994) (radiosonde releases), Cullacabardee (sodar and RASS radar), Gidgegannup (sodar to 1994), Rottnest Island (sodar, 1995), Perth Airport (twice daily sondes, four times daily winds, occasional extra sondes).

8

Creation of the meteorological fields for use by UAM involved the following steps, for each modelled hour.

6.1. Surface Temperatures

Surface temperatures were interpolated by calculating hourly-average values at each site in the measurement network, and interpolating over the data grid. Since temperatures mainly had effect through their influence on smog reaction rates, errors of a degree or so were of little concern, and this aspect of the data set was not subject to detailed review.

6.2. Mixing Depths

All possible sources of mixing depth estimates were used. These included estimates from sites where vertical temperature profiles were measured, boundary layer theory, and statistical analyses of the growth of the thermal internal boundary near the coast in unstable conditions.

Whatever the source of mixing depth estimates, it was possible to override them, or add to them. This ensured that the limitations of the mixing depth measurement systems, and lack of data in areas which might prove crucial, did not affect the creation of a consistent mixing depth field. On days when these changes or alterations were made, tests of the sensitivity of the model to them were always made.

6.2.1. Measured Mixing Depths

A mixing depth was estimated for each site and time for which a vertical temperature profile was measured. At some sites, measurements were recorded regularly through the day, while at others only a few, at intervals up to 12 hours, were available.

Where a one or two estimates for one site occurred within the hour, the estimate, or its average, could be used. However, when there was no estimate within the hour for any site, but estimates before and/or after, a set of rules was applied to determine whether they were used:

- If the model time preceded the time of the first mixing depth estimate for the day, the first was used.

- If the model time was after the last mixing depth estimate for the day, the last was used.

- If the period between the time of the last estimate before the modelled hour and the first after it was not more than eight hours, the estimate used was obtained by linear interpolation between them.

The logic behind these choices was that most sites provided at least a morning and a late-afternoon profile. Conditions did not normally change significantly before the first or after the last, but they did change in between, and there was a limit outside which interpolation was not judged acceptable.

The eight hour limit was only significant for Perth airport records, which normally included a morning and evening measurement. Occasionally, there was an extra radiosonde release at about 1 p.m.. This then permitted inclusion of airport estimates through the middle of the day.

In unstable conditions, the mixing depth was taken to be the lesser of the level where the dry adiabat from the surface temperature met the temperature profile, and the level where an onshore flow turned offshore. The latter was found necessary, to avoid the spurious loss of emissions when offshore flow above the sea-breeze inversion was wrongly represented as extending below the inversion.

Neutral conditions were taken to occur when the magnitude of the Monin-Obukhov length was greater than half the Ekman depth (defined as 0.25 u_*/f, for friction velocity u_* and Coriolis factor f). Then, mixing depth was the lesser of the level of peak potential temperature gradient in the sounding, and the Ekman depth.

In stable conditions, turbulent mixing has the effect of cooling the boundary layer. This means that temperatures rise with increasing height through the nocturnal boundary layer, falling at a fraction of the dry adiabatic lapse rate above. The mixing depth was therefore the taken from the height of peak temperature in a profile. Allowing for a region of minimal cooling at the top of the layer, in which turbulence would be close to neglible, 90% of this height was used as the estimate.

On days when data were lacking, estimates were also obtained using surface temperature measurements, and the morning temperature profile measured at Perth Airport. However, since high ozone events usually occurred on days when a cool change developed, there was often a significant trend of upper-level temperatures through the day. This meant that this approach was only reliable within an hour or two of the radiosonde release time.

Although mixing depths could not be estimated automatically from the sodar wind profiles, the wind shear evident in them was commonly valuable in manually revising the table of mixing depths. Overnight before a smog event day, the mixing depth was usually less than 200 metres. At these depths, neither the RASS radar nor the Perth Airport sonde could resolve temperature structure adequately. The sodar, with a vertical resolution of 30 metres and the ability to measure winds accurately from 30 metres upward, provided wind shear information which was the only routine source of mixing depth information at these levels.

Also used were the measurements made during ascent or descent of the FIAMS Cessna 340, during the 1994 intensive study period. Figure 5 shows temperatures averaged in layers of 10 metres' depth. It illustrates the resolution capacity of the aircraft's sensors, which provided in this case an estimate of a mixing depth which no other instrument was capable of detecting.
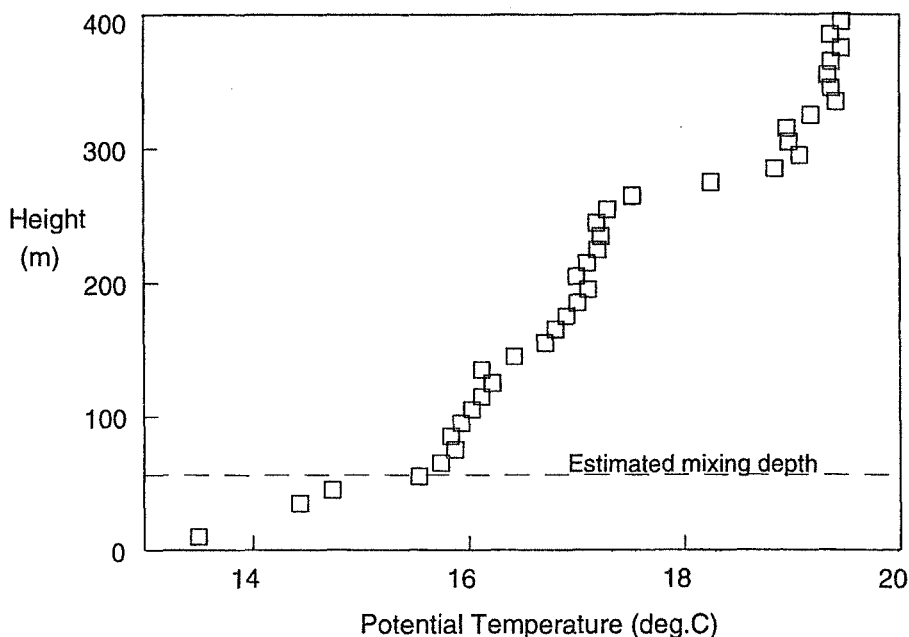
Figure 5. Temperature profile measured inland by the FIAMS Cessna 340, at 0704 on 8 February 1994 (with the Caversham 10-metre temperature added). There is a strong temperature inversion at about 270 metres, but a also shallow inversion below 50 metres.

Mixing depth estimates were then interpolated using an inverse-squares scheme. In constructing mixing depths, values offshore were presumed identical to those measured at Rottnest, and values inland were presumed the same as those measured by sonde at Gidgegannup or Rolling Green.

6.2.2. Mixing Depths Modelled from Boundary Layer Theory

In some cases - particularly over water - no reliable measurements were available. Mixing depths could then be estimated from surface layer variables, using (for consistency) the schemes employed by UAM itself, as follows.

Over water, a drag coefficient was found from

$$C_d = 0.00075 + 0.000067 \, U \tag{1}$$

where U was 10-metre wind speed. This was used as an approximate estimator of surface heat transfer coefficient, giving surface temperature flux

$$u_* T_* = C_d \, U \, (T_{sea} - T_{air}) \tag{2}$$

for sea surface temperature T_{sea} (taken to be 22°C) and measured air temperature T_{air}. Friction velocity was also derived,

$$u_* = C_d^{1/2} \, U \tag{3}$$

as was the local roughness length,

$$z_0 = z_a \, e^{-kU/u_*} \tag{4}$$

where k was von Karman's constant (0.4), and anemometer height Z_a was 10 metres. From $u_* T_*$ and u_*, the Monin-Obukhov length, L, was derived.

Over land, heat flux was approximated using measured solar radiation Q, via the equations

$$s = 3.8 \times 10^{-4} + 1.4 \times 10^{-4} \cos(\Phi) \tag{5}$$

$$h = 6.2 \times 10^{-2} + 3.1 \times 10^{-2} \cos(\Phi) \tag{6}$$

$$u_* T_* = \max(-0.03, s \, Q - 0.047 - h/2 \, \sin(2\pi t/(1 \text{ day}))) \tag{7}$$

where "s" was a correlation slope, and "h" was a morning-afternoon hysteresis term. "Φ" was the phase of the year from the summer solstice (one year corresponding to 2π radians). This was based on a relation derived during the Kwinana Air Modelling Study (Rye, 1982).

From this estimate, and the surface roughness length appropriate to the land use classification provided for use by UAM, u_* and L were found using surface-layer relationships.

In either over-land or over-water conditions, the derived surface layer parameters define two mixing depths estimates. For neutral conditions, the Ekman depth was taken to be 0.25 u_*/f (where "f" is the Coriolis factor). A stable-conditions estimate was based on the Zilitinkevitch (1972) expression, with a proportionality constant as modified by Brost and Wyngaard (1978), in the form $0.4 \, (u_*/(|f|L))^{1/2}$.

6.2.3. Thermal Internal Boundary Parameterisation

For cases where limited mixing depth measurements were available, it was necessary to impose some form of thermal internal boundary layer (TIBL), for onshore flows. The approach used was to determine an inflow lapse rate. The mixing depth at any grid point could then be found from the temperature rise between the coast and the grid point.

Two methods of defining the lapse rate were used. In the first method, the lapse rate was derived using measurements made by the DEP at the coast near Kwinana. These have included aircraft passes inland in sea-breeze conditions, in conjunction with continuous surface monitoring (Rayner, Bell and Watson, 1990). Twenty one such cases were analysed using principal component analysis (e.g., Gonzalez and Wintz, 1987, p. 122-125). For inflow potential temperature lapse rate, the best fit was found to be given by

$$\lambda \quad = \quad -0.017514 \cos(2\pi t/(1 \text{ day})) + 0.003624 \, T - 0.004117 \, u +$$

$$0.003817 \, u_{off,max} - 0.085558 \tag{8}$$

for λ in $^{\circ}C \, m^{-1}$, where t was time of day, T was air temperature ($^{\circ}C$), u was onshore wind velocity, and $u_{off,max}$ was the maximum measured offshore wind preceding a sea breeze (both in ms^{-1}). For this relationship, the correlation coefficient (r^2) was 0.75. Measurements at the Swanbourne monitoring site were used to define T, u and $u_{off,max}$.

With a defined lapse rate, the mixing depth was then estimated using

$$H \quad = \quad 1.2 \, \Delta T_i \, / \, \lambda$$

where ΔT_i was the inland temperature rise, and the factor 1.2 included a correction for turbulent entrainment at the inversion base (e.g., Deardorff 1980).

The other approach was to specify an hourly table of inflow lapse rates. This was useful for parametric studies, and in one case where adequate base data for the the above approach were not available.

6.3. Wind Velocities

In principle, there were three wind profile estimates available for each site. Wind speed measured at 10 metres, and Monin-Obukhov length, together gave a surface-layer profile. For the mid regions of the boundary layer, boundary layer winds were estimated, based on the work of Hess, Hicks and Yamada (1981).

This scheme was dependent on the stability parameter,

$$S \quad = \quad \frac{k \, u_*}{|f| \, L} \tag{9}$$

If S was of magnitude less than 10, neutral conditions were assumed appropriate, giving the wind speed functions (after Hess et al., equation 16)

$$<U> \quad = \quad \ln(H/z_0) - 1.1 \tag{10}$$

$$<V> \quad = \quad 4.3 \tag{11}$$

for mixing depth H. In stable conditions, for S above 10, the expression proposed by Hess et al. (their equations 17 and 18) was

$$<U> \quad = \quad \ln(H/(z_0 \, S^{1/2})) + 0.96 \, S^{1/2} - 2.5 \tag{12}$$

$$<V> \quad = \quad 1.15 \, S + 1.1 \tag{13}$$

In the model, an additional wind profile factor was estimated in stable conditions, of form

$$<U'> \quad = \quad 116 \, (H/(200 \, L))^{1/2} \, (z' - z'^2 - 0.18) \tag{14}$$

$$<V'> \quad = \quad 57 \, (H/(200 \, L))^{1/2} \, (1.4 \, z' - z'^2 - 0.51) \tag{15}$$

12

where z' = z/(200 L) for plume height z, added to <U> if it was positive. This formulation represented the nocturnal-jet profile apparent in the figures 14 to 16 of Hess et al.. Although it was not certain that the same form of nocturnal wind profile would prevail elsewhere, cases of significantly stronger winds at levels above 100-200m have been observed on the Perth coastal plain, and some form of representation was therefore felt necessary.

In unstable conditions, for S less than -10, the function used was, after Hess et al.,

$$<U> \quad = \quad \ln(-L/z_0) \tag{16}$$

$$<V> \quad = \quad k / 0.25 \tag{17}$$

where the latter was based on a presumption that mixing depth was about 0.25 of the Ekman scale length, $u*/|f|$.

The along-gradient-wind and across-gradient-wind boundary layer wind speed estimates were then taken to be

$$U \quad = \quad \frac{U_*}{k} <U> \tag{18}$$

$$V \quad = \quad \frac{U_*}{k} <V> \tag{19}$$

Interpolation of a three-dimensional wind field involved the following stages:

- A horizontal wind field was interpolated, using available vertical wind profiles and a selection scheme identical to that for mixing depth. Due to the direct measurement of winds, however, no manual adjustments of estimates were made.

- Next, a surface (10-metre) wind field was interpolated from surface measurements.

- The surface wind fields, and heat flux estimates based on measured insolation, were used to derive Monin-Obukhov length and friction velocity for each site. Based on the work of Hess, Hicks and Yamada (as above), a representative boundary layer wind velocity was then estimated.

- The final wind velocity profile for each grid point followed a linear trend from the surface layer profile at the surface, to the boundary layer value at half the mixing depth, then a linear trend from the boundary layer value to the interpolated windfield at the mixing depth.

- Some divergence compensation was then introduced. Because of the near-straightness of the coastline, the majority of the convergence in the model occurred in the west-east direction. This allowed divergence compensation to be applied in a one-dimensional sense, with west-east convergence at the surface balanced by west-east divergence aloft, and the slight amount of south-north surface convergence balanced by south-north divergence aloft.

   The scheme used presumed greatest accuracy for the surface wind field. Convergence within the boundary layer was calculated at each point, and a divergence correction giving zero total convergence was applied. This increased linearly through the boundary layer, from zero at model layer 1.

Temperature gradients above and below the diffusion break were estimated for each temperature profile site, using the same selection criteria as for mixing depth and wind velocity. It was found, however, that use of the actual gradient above the inversion (as recommended in the documentation) gave unrealistically high temperatures when extrapolated

13

to the top of the modelled region. This caused reaction rates to become unrealistically large, drastically slowing the model's calculations. As a result, the temperature gradient above was based on the temperature and height differences from the inversion base to the top of the modelled region.

There was provision in UAM for only one temperature gradient above, and one below, the inversion at each hour of the modelled period. The location used was that of the air mass located at model level one, at the centre of the business district at 8 a.m. and before, and following the level 1 wind trajectory afterward.

7. Initial and Boundary Conditions

Data from a configuration file, which included side and upper boundary concentrations for all modelled species, was normally used to generate the required files. Alternately, the final output records from one run of the model could be used to generate a set of initial concentrations, to initialise a run for later days of a multi-day smog event.

8. Model Output Parameters

UAM calculates the time and spatial evolution of 24 chemical species, including ozone, oxidised nitrogen compounds, and a range of ROC groups. These are written to an hourly data file, for later review.

A post-processing program was created to interface the model output to local graphics hardware, and to allow detailed analysis and comparison with measurements. An important element of this software was integration of the Integrated Empirical Rate (subsequently termed "IER") algorithm into processing of both the modelled and measured concentrations.

This scheme (Johnson, 1984) allows the presentation of results in a manner which can separate the influences of nitrogen oxide and ROC emissions. This provides a valuable tool in any review of model calculations, because discrepancies in modelled results can be due to errors in meteorological fields, nitrogen oxide or ROC emissions. Any mislocation of the ozone peak can usually be attributed to errors in meteorology. But an error in ozone concentrations can be due incorrect mixing depths, or to errors in estimates of either nitrogen oxide or ROC emissions. The IER parameter "SP_{max}", which corresponds to the theoretical maximum smog which may be produced, has the advantage of responding only to nitrogen oxide emissions. Comparison of errors in ozone and SP_{max} values has proven a crucial step at many points of the model validation process.

9. Case Studies

The Urban Airshed Model was applied in analysis of ozone events on several days through the Study. The particular days reported here, and the motives for selection of each, were as follows:

4 February 1994: the day of the ozone event for which the most detailed validation data were collected during the Study.

19 February 1994: a major example of a "coastal" smog event.

16 March 1994: a day when an "inland" smog event occurred, used to analyse the sensitivity of the model to vehicular emissions.

18 March 1994: similar to 16 March 1994, but with more southerly winds associated with a slow-moving sea breeze front, used to test the sensitivity of model results to emissions from the Kwinana area.

21 March 1994: the event for which fair validation of modelled meteorological fields was most readily obtained, used to investigate the differences in model results based on measured and modelled meteorology.

8 January 1993: another "inland" event, the day of highest ozone concentrations during the Study, also used to investigate the role of biogenic ROC and Kwinana industrial emissions in the development of peak ozone concentrations.

13 January 1993: a day when high ozone concentrations were due to the interaction of ROC in bushfire smoke with urban and Kwinana emissions.

9.1. 4 February 1994

This was the day of most intensive field monitoring, during the 1994 summer field exercise. While lower than normal temperatures ensured that peak ozone concentrations were moderate, at about 60 ppb, the meteorology of the day was close to that typical of more significant smog events. Peak SP_{max} values showed that, in warmer conditions, ozone levels could have reached the vicinity of 100 ppb.

The primary objective in modelling this day was to determine the accuracy limitations of the modelling system - including both the meteorological data preprocessor and UAM itself - in conditions of optimum data availability.

9.1.1. Data Used

Since the day's meteorology was typical, the preselected measurement sites were located close to the track of the main mass of emissions. With measurements made at these locations, and additional ones taken on the day, it was possible to model the event using measurements alone.

The modelling process highlighted a number of issues. In the interests of formalising the lessons learnt, and of scientific rigour, these are detailed below:

● Initially, velocity convergences within the boundary layer were compensated by divergence in the layers above, but this approach saw significant loss of smog from the boundary layer. With hindsight, it was felt that the top of the boundary layer should form a barrier to pollutant motion. The compensation scheme was therefore changed, surface-level convergence being compensated by a correcting divergence within the boundary layer, increasing linearly from zero at the first model level.

● The Swanbourne outflow of nitrogen oxides could initially not be modelled accurately, using only radiosonde and radar mixing depth estimates. A single estimate of about 100 metres, for Swanbourne at 6 a.m., suggested other inland measurements might have had inadequate height resolution at low levels. Subsequent analysis of aircraft measurements confirmed this belief. When aircraft measurements were added to the data set, and estimates apparently invalid due to the lack of low-level detail were removed, the level of agreement was much improved.

Table 1 summarises the additional mixing depth measurements used. The availability of the aircraft values over water in the period 8 a.m. to 12 noon should be noted. In particular, the 130 metre value at 10:07 a.m. provided an explicit measure of the stability of the initial sea breeze inflow. (See Figure 6).

Location	Time	Mixing Depth	Method
Perth Airport	06:16	200	Radiosonde
	07:09	210	Aircraft
	12:13	475	Radiosonde
	12:57	430	Aircraft
	18:22	807	Radiosonde
Rottnest Island	05:58	241	Radiosonde
	08:40	180	Aircraft
	12:00	150	Aircraft
	14:97	511	Radiosonde
Swanbourne	05:59	97	Radiosonde
	09:33	190	Radiosonde
	10:07	130	Aircraft
	11:98	197	Radiosonde
	15:00	380	Radiosonde

Table 1. Mixing depths measured using radiosonde or aircraft ascents/descents on 4 February 1994.

The mixing depth implied by the 9 a.m. sonde release from Rottnest, of about 500 metres, has been deleted from the list in Table 1. While this sounding showed a strong inversion at about 500 metres, there was some stability below this level, and the 500 metre value was well in excess of other estimates at about this time. On the other hand, the aircraft sounding (taken over water near Rottnest) revealed a stable layer commencing between 150 and 200 metres (Figure 7).
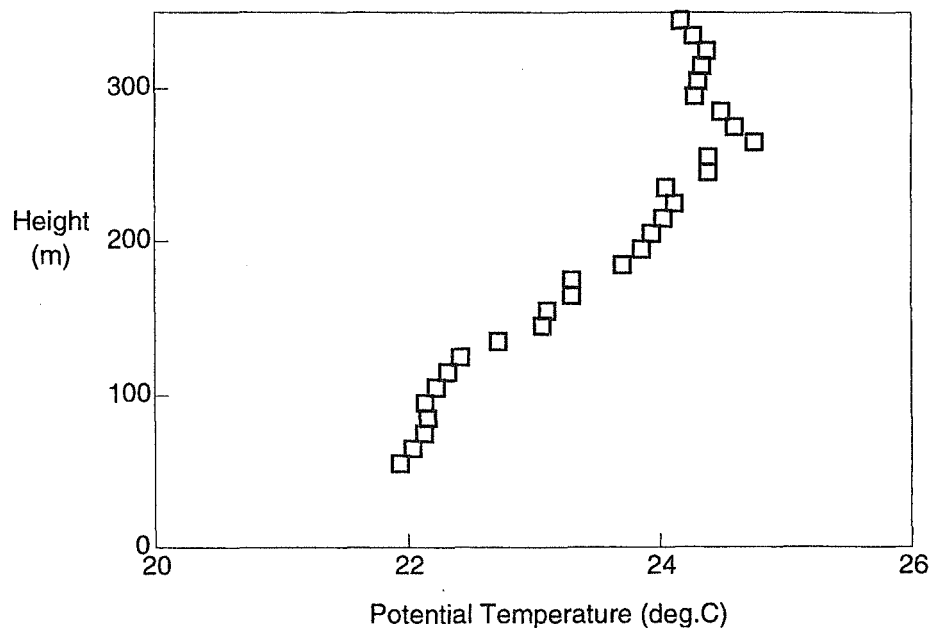
Figure 6. Temperatures measured by the Flinders University aircraft offshore from Swanbourne, at 10:07 a.m. on 4 February 1994. The "potential temperature" shown here is actually temperature + (0.00977 °C m^{-1}) x height. The stable layer below 250 m corresponds to the sea breeze inflow.

Height (m)

300

200

100

0

20.0   20.5   21.0   21.5   22.0

Potential Temperature (deg.C)
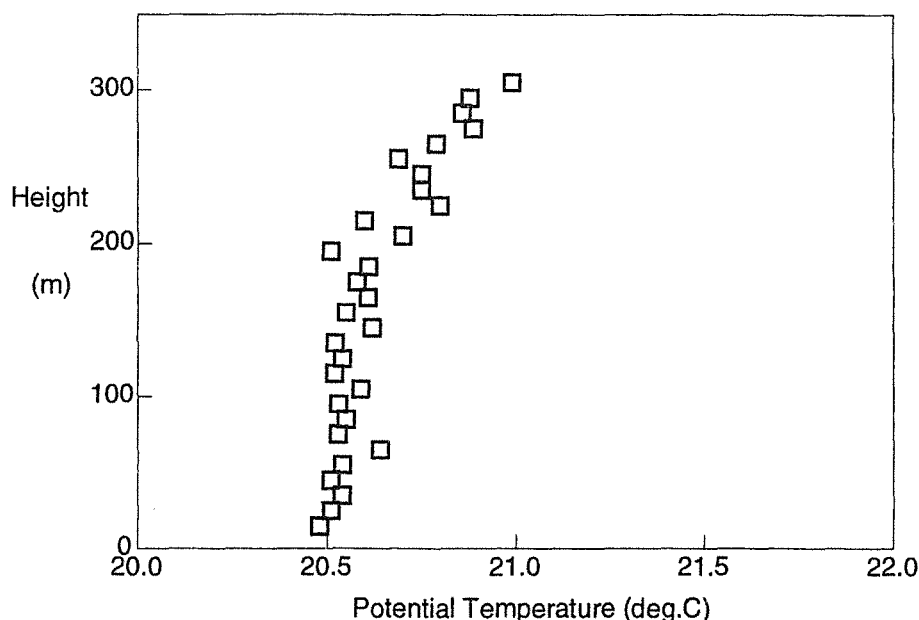
Figure 7. Potential temperature profile measured by the Flinders University aircraft near Rottnest, at 8:40 a.m. on 4 February 1994.

- While total nitrogen oxides were well represented, there was an overestimation of the quantity of nitric oxide, and an underestimation of nitrogen dioxide. Whether this is due to an incorrect subdivision of tailpipe emissions, or to an underestimation of the conversion rate by UAM, is not known.

- The passage of the main ozone mass was followed, at Caversham and Cullacabardee, by a couple of hours of lower, but still increased, concentrations. These were due to the later return of the emissions which moved offshore in the early morning. However, using the initial interpolated windfields, the morning emissions passed, on return, south of these sites.

To reproduce the general form of the time dependence of ozone at these sites, it was found necessary to impose a slight permanent southerly component offshore of Rottnest Island (where the westernmost measurement point was located). Such a wind was expected to have been present, but there were no data to provide an explicit measure of its strength or direction.

- Initial runs were conducted without inclusion of any biogenic emissions, and the result showed very little smog production. Use of the emissions factors of Guenther, Zimmerman and Wildermuth (1994) produced emissions well in excess of expectations, resulting in significant overestimation of measured ozone concentrations.

The emissions factors were replaced by those of Lamb, Gay and Westberg (1993), but reactivity before the onset of westerly flow was still overestimated. Normally, a factor of 0.5 was applied to biogenic emissions, to give approximately the correct pre-sea breeze reactivity.

9.1.2. Review of Model Results

Although there was high confidence in the validity of the meteorology and emissions used for this day, accurate representation of the ozone peak was not readily achieved. Figure 8 shows a comparison of measured and modelled ozone concentrations for three representative sites on the day. The general trends of background concentrations were well represented, but the peak
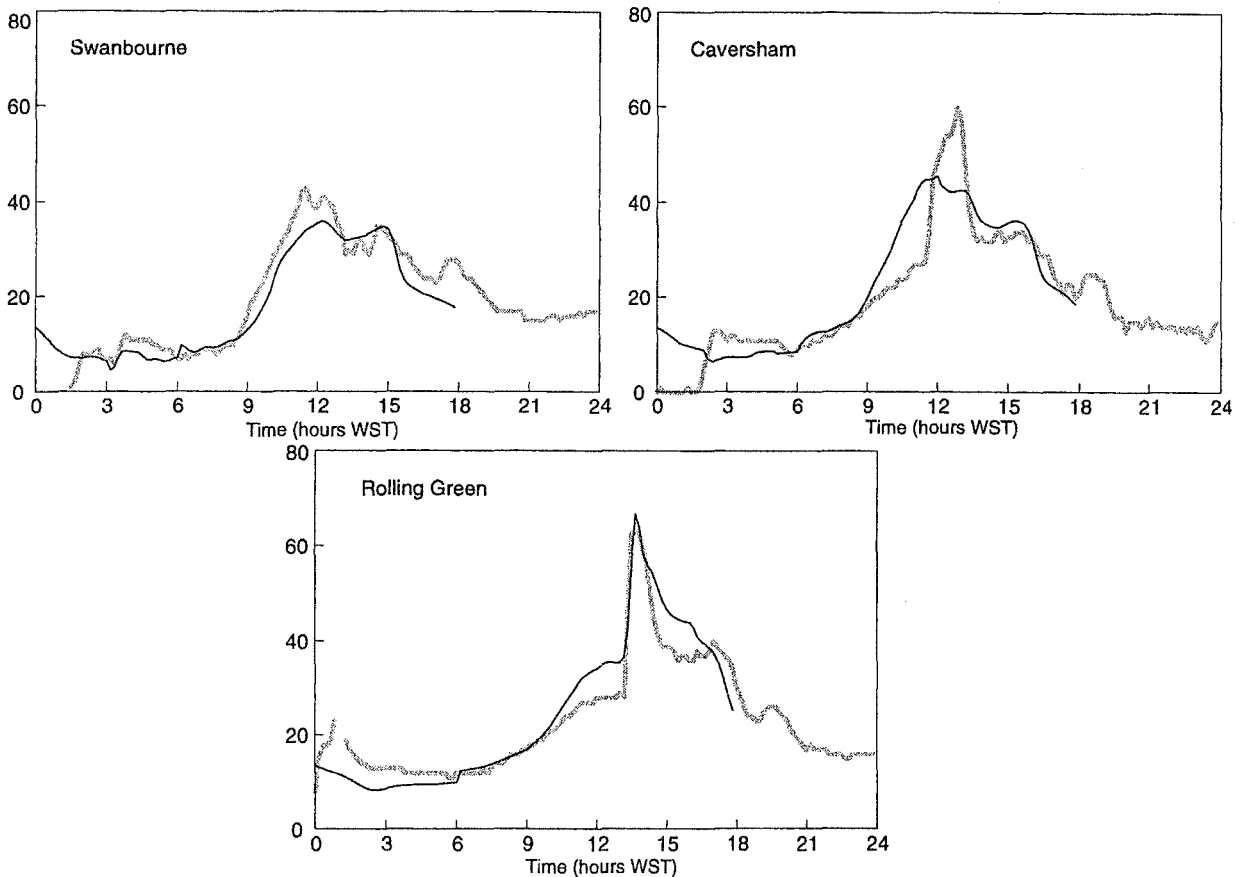
Figure 8. Ozone concentrations (ppb) for the Swanbourne, Caversham and Rolling Green sites on 4 February 1994. The solid lines represent modelled results, the shaded lines measurements.

concentration (coinciding with the passage of the sea breeze front) did not develop, except well inland at Rolling Green.

Reasons for this shortcoming received extensive investigation. The availability of nitrogen oxides to supply the ozone reactions was tested by comparing modelled and measured concentrations at Swanbourne (Figure 9). Given the level of agreement shown in this figure, and the confidence in mixing depths estimates based on radisonde and aircraft measurements, the supply of nitrogen oxides was not considered an issue.

Review of the SP_{max} trend at Caversham (Figure 10) showed better agreement in the crucial time period, although the modelled concentration decreased more rapidly after the passage of the sea breeze front. This implied that the major reason for the absence of the ozone peak was the failure of reactions to progress in the conditions modelled - particularly, between the coast, and inland sites. This possibility was supported by the better validation at Rolling Green, where photochemical reactions had completed in both modelled and measured cases.

A weakness of UAM in conditions of low temperature and low ratio of hydrocarbon to NO_x emissions has been observed previously (e.g., Azzi, Johnson and Cope, 1992, Figure 1). The relevance of this to the 4 February 1994 event was tested by re-running the model, with all air temperatures increased by 5°C, but there was no major improvement in results.

18
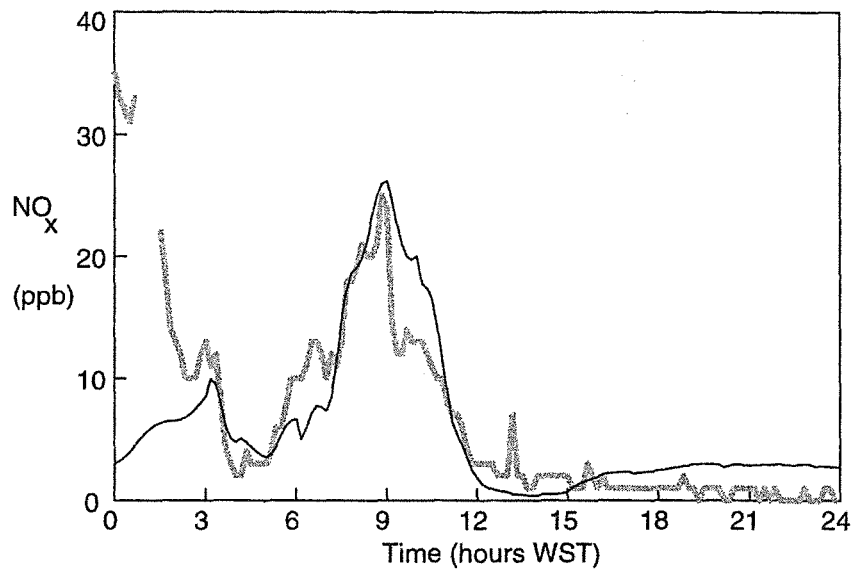
Figure 9. Concentrations of NO_x (NO + NO_2) at Swanbourne on 4 February 1994. The solid line represents modelled results, the shaded line measurements.

Review of the vehicle inventory of emissions of ROC (James, 1995) showed an estimated vehicle hydrocarbon emission rate of about 80,000 kg day^{-1} in 1994. During peak traffic times, hourly emissions were 6.71% (7-8 a.m.) and 7.77% (8 to 9 a.m.) of the total - i.e., 5370 and 6220 kg/hour, or about 1.5 and 1.7 kg s^{-1}. These compared well with aircraft measurements of total urban emissions, in the range 0.8 to 2.5 kg s^{-1}, averaging 1.7 (Carras, et al, 1994). The accuracy of the ROC inventory, and calculations based on it, is considered further in section 9.3.2.
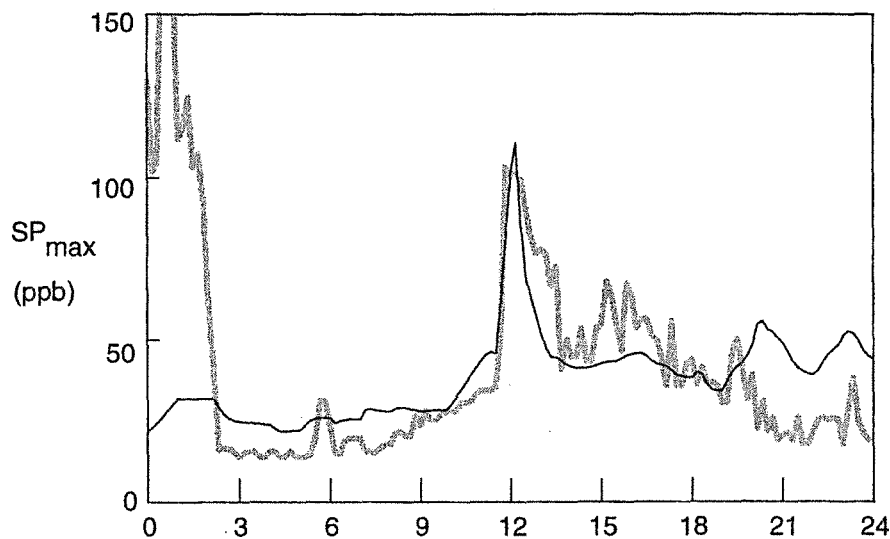
Figure 10. SP_{max} concentrations for the Caversham site on 4 February 1994. The solid line represents modelled results, the shaded line measurements.

9.2. 19 February, 1994

This day was an extreme case of a class termed "coastal events", in which high concentrations of ozone occurred at the coast, but with lower values being measured inland. Unlike other events studied, the reactivity of urban emissions was not a significant factor, since both model and measurement showed smog reactions completed well before the smog mass returned to the coast. The data set did, however, provide a good test of the ability to model an event when the smog-bearing air mass passed through a data-sparse region.

9.2.1. Data Used

The meteorology of the 18 February was in the range of conditions with potential to contribute to smog on the next day, so radiosonde teams were deployed at Rottnest Island and Swanbourne. This meant that data availability was close to its maximum.

However, the easterly airflow overnight carried the preceding evening's emissions past Rottnest Island beween 1 a.m. and 6 a.m. (See Figure 11). Presumption of a uniform windfield west of Rottnest, matching winds at Rottnest, suggested the trajectory of air returned to the coast in the afternoon may have extended as much as 100 km offshore.

This meant that much of the evolution of the smog occurred within a region from which almost no data were available - the only exceptions being ship wind reports, of calm conditions 80 km west of Bunbury at midnight, and 5-10 knots south to south westerly about 200 km west of Geraldton, at 8 a.m. and 2 p.m.

These reports did, however, confirm surface chart suggestions of very light winds near the trough axis, so that little dispersion of the plume was likely. This meant that vertical wind shear was likely to be of minor concern, simplifying the task of estimating meteorological conditions in the poorly-known region. They also suggested the trough axis during the morning period should be at least 100 km offshore, and probably not more than 150 km offshore.

The main smog mass was detected returning past Rottnest, at a well defined speed, at 3 p.m.. Some initial trajectory estimates showed that, in order for the plume to return at the time and place it did, there was little freedom to adjust windfields away from a fairly normal pattern. The optimum initial trough location proved to be about 120 km offshore, with a 2 m s^{-1} south easterly on its seaward side, and a 2 m s^{-1} north easterly on the landward side. These values were maintained until 11 a.m., with uniform winds matching those at Rottnest taking over at noon.

Given these presumptions, the day posed several questions related to the occurrence of offshore smog events, namely:

1. Was it possible to model, to any degree of accuracy, the concentrations returning onshore? Given that only winds had been matched to give the correct return time, how sensitive to initial presumptions of mixing depth was the result?

2. What was the relative contribution of Kwinana emissions likely to have been, and what level of certainty could be attached to the estimate?

3. How far inland did elevated ozone concentrations persist?

9.2.2. Model Results

Once a reasonable match of arrival time of the main ozone peak at Rottnest was achieved, the model was run for three different choices of mixing depth in the trough region. Of the values chosen, the first (500 metres) was greater than those normally measured, the next (300 metres)

was similar to those measured, and estimated in typical numerical modelling, and the last (200 metres) was in the low range of those which might have persisted in light winds.

Calculations showed respective peak ozone concentrations returned in the vicinity of Rottnest Island of 95, 110 and 75 ppb. The last of these was reduced because the returning plume, generated by the previous day's emissions, followed a more northerly trajectory. This meant it interacted less with modelled day's emissions. There was a clear indication that the likely wind and mixing depth combination was in the optimum range for an ozone event.

The time sequence plot for NO_x concentrations at Rottnest Island (Figure 11) showed high concentrations in the overnight offshore flow, particularly at the plume axis, which was modelled as passing about 10 kilometres to the north of the measurement site.
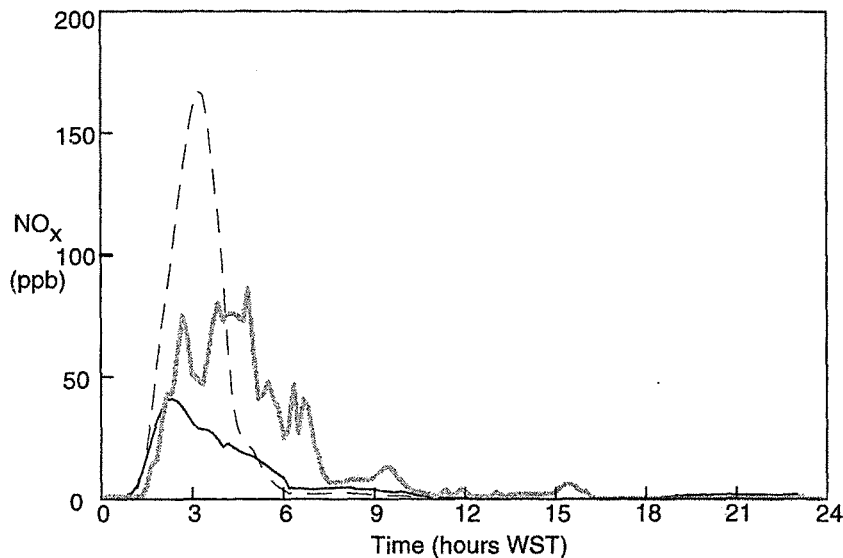
Figure 11. NO_x concentrations for 19 February 1994. Wide shaded line line - measured at Rottnest, solid line - modelled for Rottnest, broken line - modelled at the urban plume axis

The level of agreement between peak concentrations is arguable, given the steep north-south concentration gradient evident at Rottnest Island in Figure 12. However, the longer duration of measured concentrations, compared to those modelled, is clearly an issue.

Probably related to this is a comparable discrepancy at the Caversham site, where NO_x concentrations were measured as decreasing from 80 ppb to 25 ppb, from midnight to 6 a.m., while modelled concentrations decreased from 50 ppb to 10 ppb. Winds at the time were light easterlies. Trajectories to Caversham near midnight, based on surface winds, suggested a source region in the foothills of the Darling Scarp.

A possible cause would be an undetected katabatic flow at the Darling Scarp, recirculating urban emissions drifting inland at a higher level. This would have resulted in the escape of less urban NO_x inland, and a longer-duration outflow of higher peak concentration.

The time variation of modelled ozone concentrations at Rottnest Island is shown in Figure 13. The modelled peak arrived a little before the time of the measured peak, with a slightly lower maximum and a slightly lesser duration.

However, while this comparison looks superficially good, the differences between measurement and model are significant, and comparisons at other sites were not as good. Peaks in the vicinity of 120 ppb were also detected at Swanbourne and Two Rocks (Quinns

21
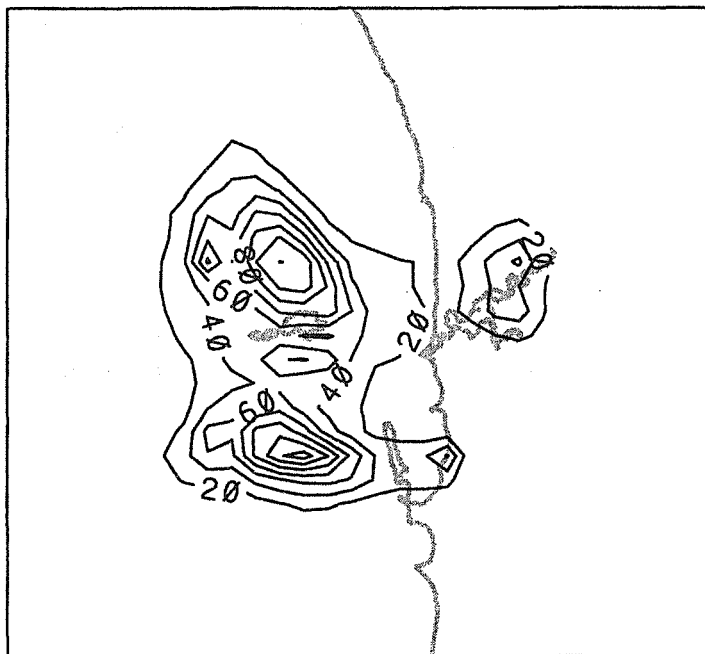
Figure 12. Modelled NO$_x$ concentrations (ppb) at 3 a.m. on 19 February 1994

Rocks being out of action on the day). Modelled peaks at the coast were much less (Figure 14).

It appears probable that, due to the longer duration of the actual NO$_x$ outflow overnight, the pool of ozone forming at the trough was broader, or of higher concentration. Based on the comparison in Figure 11, the discrepancy might have been as high as a factor of two, although indications from similar measurements at Swanbourne suggested a lower value.

A further notable difference is the presence of a significant "tail" of ozone concentrations in the modelled results, while measured concentrations dropped quickly to background. This is evident in Figure 13 as a less sharp drop after the modelled peak, and also in Figure 14 as slightly increased peak ozone concentrations west of the trough axis. The effect may have been due to entrainment of some of the elevated NO$_x$ into this region in the model, without a parallel occurrence in fact. The low vertical resolution used in the layers above the mixing depth may have contributed to the discrepancy.

Notwithstanding these differences, the modelled event remained a feasible occurrence - perhaps a more probable combination of events, given that some of the discrepancies may have been due to extreme circumstances on the actual day. This meant that the day remained a useful "generic" analysis day.

9.2.3. Sensitivity Studies

Because the smog reactions were essentially complete when the peak arrived at the coast, the main sensitivity issues of relevance on this day related to the relative contributions of various NO$_x$ sources. The main two potential sources were the urban region, and Kwinana industry.

The model run was repeated with all sources in the Kwinana region set to zero. A source was taken to be in Kwinana if it lay within the range of AMG northings 6429 and 6440 km, and west of AMG easting 387 km. Significantly, there was no appreciable change of peak ozone concentrations except near Kwinana itself.

22
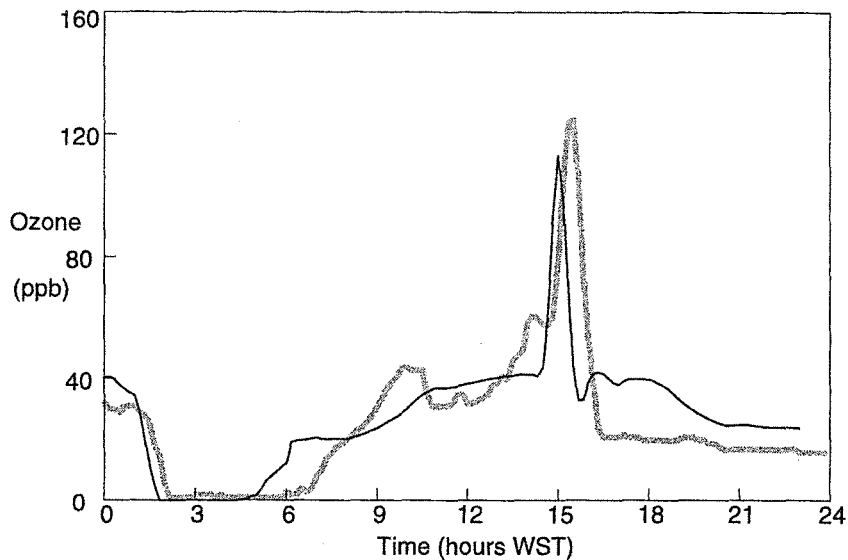
Figure 13. Ozone concentrations at Rottnest Island on 19 February 1994. The wide shaded line represents measurements, the thin black line model calculations.

Trajectory analyses showed the reason to be the persisting northerly winds in the region between the trough and the coast, in the morning. This meant that the transition to the sea breeze occurred with wind directions passing through north, rather than through south. Kwinana emissions therefore were carried to the south, away from the main returning smog mass.

The consequence can be seen in Figure 14, as a broad area of peak instantaneous concentration from 60 to 70 ppb, near the coast in the south of the modelled region. The small peak over 70 ppb in the centre of this area is of concern, given that on this day the modelled
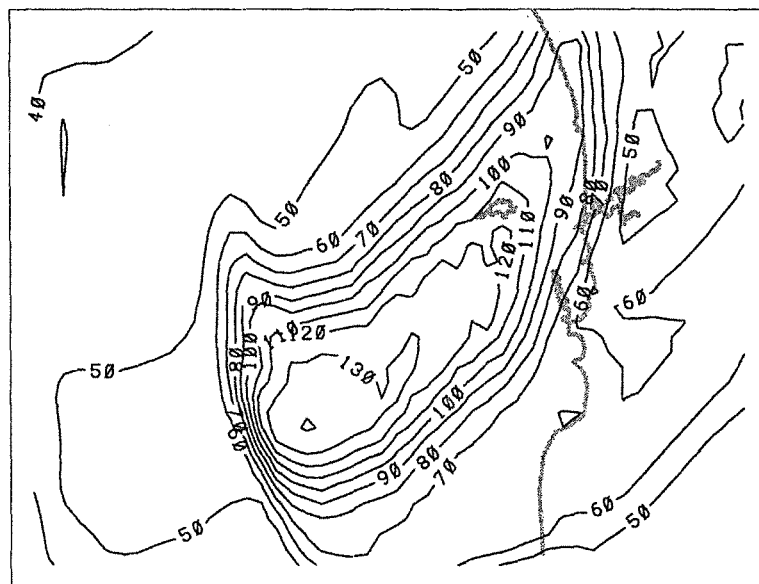
Figure 14. Modelled instantaneous peak ozone concentrations for 19 February 1994. The peak offshore is due to the production of ozone at the trough axis, in the morning.
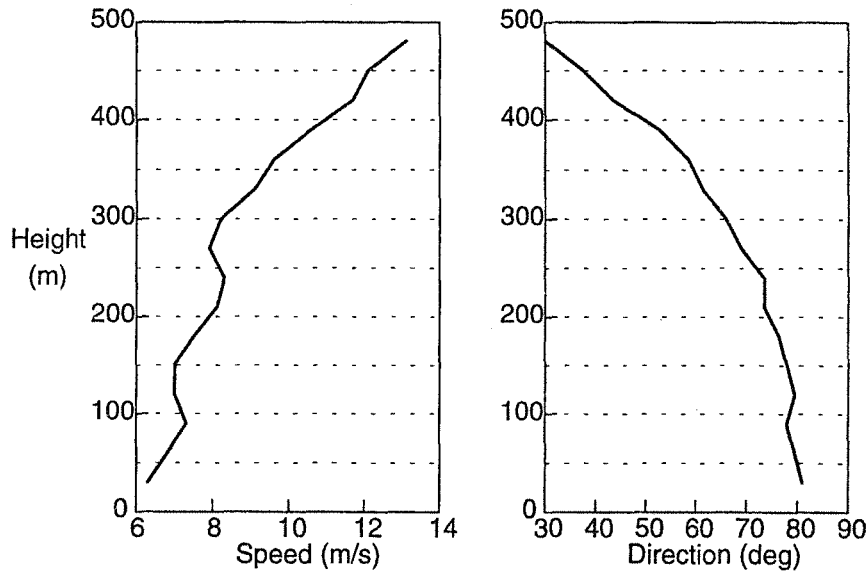
Figure 15. Wind speeds and directions measured by the Cullacabardee sodar at 0930 WST on 16 March 1994. Decreased shear of both wind speed and direction below 250 metres suggested a mixing depth of 250-300 metres.

coastal ozone concentrations at the Perth coastline underestimated the hourly average peaks there.

9.3. 16 March 1994

Weather for the period from 16 to 21 March 1994 was dominated by a weak low pressure trough, held in position by the effects of a tropical cyclone to the north of the state. Significant events occurred on 16, 17, 18 and 21 March.

The smog event on 16 March was particularly relevant, because it highlighted issues related to the emissions inventory which will require further study.

9.3.1. Data Used

Previous records had shown no significant smog events after the first week of March, and as a result the detailed field monitoring programme had been ended. This meant that radiosonde observations from Swanbourne and Rottnest were unavailable. The shortage of vertical profile data was compounded by the failure of the Cullacabardee RASS temperature system. Only the Perth Airport radiosonde gave a usable temperature profile, although the Cullacabardee sodar and radar both provided wind profiles.

In order to add detail to the mixing depth record, the wind profiles were analysed carefully for shear layers, and other evidence indicative of the mixing depth. The sodar, with high resolution from a height of only 30 metres, was particularly useful for this task. The analysis involved study of each half-hourly record of a day, for trends with both time and height. Figure 15 illustrates one aspect of the analysis, at a time when convection could be expected to reduce shear within the mixed layer.

Analysis was simplified by the observation that the previous evening's emissions were lost from the metropolitan region, so that the event only involved emissions at the time of the morning peak hour and later. Since evening concentrations were also not of interest, most model runs therefore commenced at 7 a.m. and ended at 6 p.m.

9.3.2. Model Results and Sensitivity Studies

Figure 16 shows the ozone concentrations at Caversham, calculated by three runs of the model using identical meteorological data.

The first run used

• vehicle emissions as in the inventory ("high oxidant day" estimates)

• area-based emissions as in the inventory

• biogenic emissions half the inventory estimates

• industrial emissions as in the inventory, with the exception of Kwinana ROCs, which were increased by a factor of three (See section 4.3)
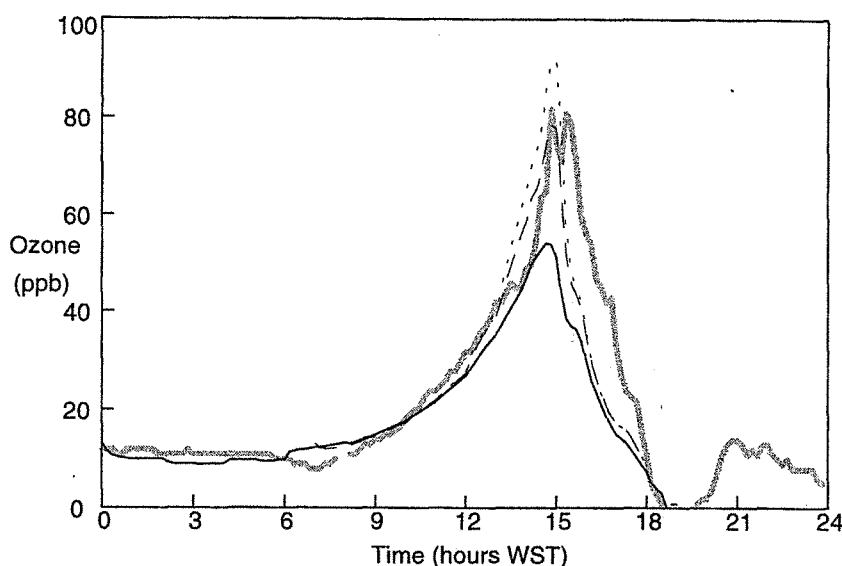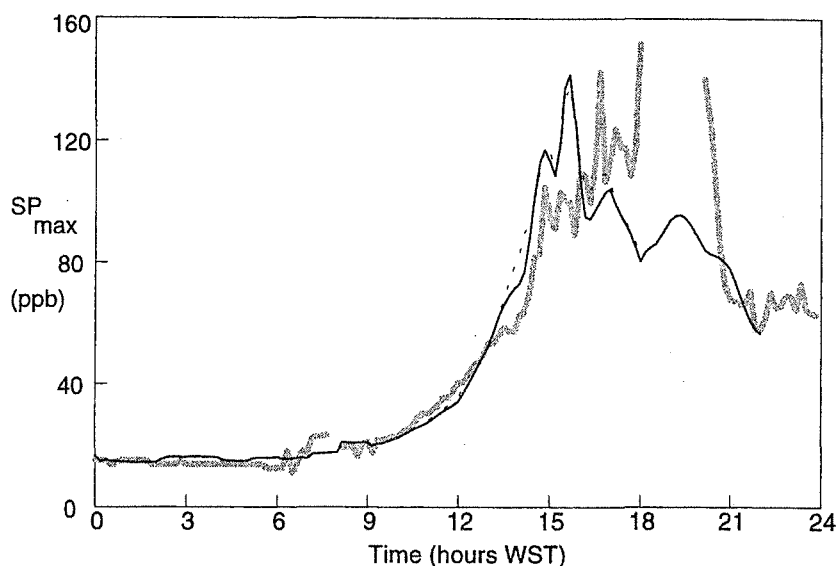

Figure 16. Measured (wide shaded line) ozone concentrations for Caversham compared with model results, for 16 March 1994. The solid line is for inventory vehicle ROC emissions, the dashed line for 1.6 times inventory values, and the dotted line for 2 times inventory values.

Since the day was characterised by high inland ozone concentrations, analysis concentrated on comparisons between model calculations and measurements at Cullacabardee, Caversham and Kenwick.

In spite of careful review of meteorological inputs, it initially proved impossible to obtain a close match between measured and calculated ozone concentrations at any site except Kenwick.

The first check used the IER model's SP_{max} estimator, to test the accuracy of the combined meteorological and NO_x inputs. Figure 17 compares SP_{max} calculated for Caversham from model output with that found from measurements, for two levels of vehicle ROC emissions.

This indicated that the smog-forming potential of the air passing Caversham in the crucial afternoon period was well represented. In turn, the result implied that either the vehicular NO_x and meteorological estimates were accurate, or that errors in each compensated. Experience with several other modelled events also supported the accuracy of vehicular NO_x estimates, so the former was taken to be the case.

160

120

SP
  max

80

(ppb)

40

0

0   3   6   9   12   15   18   21   24

Time (hours WST)

Figure 17. Measured (wide shaded line) SP$_{max}$ concentrations for Caversham compared with model results, for 16 March 1994. The solid line is for inventory vehicle ROC emissions and the dotted line for 2 times inventory values.

The difference between the accuracy of calculations for Kenwick and those for other sites appeared due to differing smog sources. Kenwick received its ozone peak from emissions produced by the Kwinana industrial area, while the other sites received urban emissions. The sensitivity of model results to urban ROC emissions - primarily from motor vehicles - was therefore tested.

Figure 16 shows, as well as the base run variation, the changes of ozone through the day at Caversham, for vehicle ROC emissions increased by factors of 1.6 and 2. Clearly, best agreement would be achieved by a factor in the range 1.6 to 1.8 - although, taking into account the slight overestimation of SP$_{max}$ at the time of the peak (Figure 17), a ratio close to two might have been more appropriate. A similar ratio was implied by the Cullacabardee comparison.

The value of this result is, nevertheless, not clear. The Carbon IV chemistry model used in UAM has a known weakness in conditions of low ROC / NO$_x$ ratio (Azzi, Johnson and Cope, 1992, Figure 1). The Perth emissions inventory was adjusted to accommodate the effects of high summer temperatures, but still estimated the mass of vehicular ROC emissions (tailpipe plus evaporative losses) as just under double NO$_x$ emissions. Converting to volume fractions involved dividing the ROC emissions by a molecular weight of 0.0139 and the NO$_x$ emissions by the molecular weight of NO$_2$, 0.046, giving a ratio close to six.

This was closer to the lower of the ratios 4.8 and 10.8 for which results were quoted by Azzi et al. (1992). For the former, the reactivity calculated by the Carbon Bond IV model was roughly half that measured. Further study of Figure 1 of Azzi et al. showed that the failure of the Carbon Bond IV model may have been due to an inadequate response of the modelled reactivity to increased temperature.

A reasonable conclusion is that the conditions prevailing within the Perth metropolitan area are in a regime of weakness of the Carbon Bond IV model, and that reactivities will be underestimated significantly.

26

An adjustment factor of two on vehicular ROC's may permit study of the sensitivity of ozone concentrations to NO_x emissions. However, any increase of ROC emissions would be expected to take the modelled conditions out of the regime of weakness of Carbon Bond IV, giving a disproportionate increase in modelled reactivity. This means that, if the ratio of two is used as a start point in future studies, the effect of changes to ROC emissions may be overestimated.

Figure 17 demonstrates the applicability of the IER model at Caversham. In spite of a doubling of vehicular ROC emissions, and a corresponding large increase in peak ozone concentrations (Figure 16), SP_{max} values were hardly altered.

Also evident in Figure 16 is a shortfall of ozone concentrations in the period from 3 to 6 p.m. (hours 15 to 18). Figure 17, on the other hand, shows much better agreement in SP_{max} concentrations. This error is a common feature of events modelled in this study, and corresponds to the period of the day when back-trajectories passed over the Kwinana region. It is possible that, due to rapid temperature rises about noon, when the air passed over Kwinana, the emissions of ROCs from storage tanks were increased. This could require enhancement of the emissions inventory by more than the standard factor of three used in these calculations.

The overall pattern of ozone concentrations, for all emissions combinations, showed several features (Figure 18). There is a clear line of peak ozone concentration, parallelling the alignment of the sea breeze front. A peak near its northern end corresponded, in this case, to urban emissions which accumulated during a calm period just before midday. The southern region comprised the returned urban morning emissions, with some Kwinana contribution. Between these regions was a region where concentrations were reduced by the incursion of a NO_x plume from Kwinana.
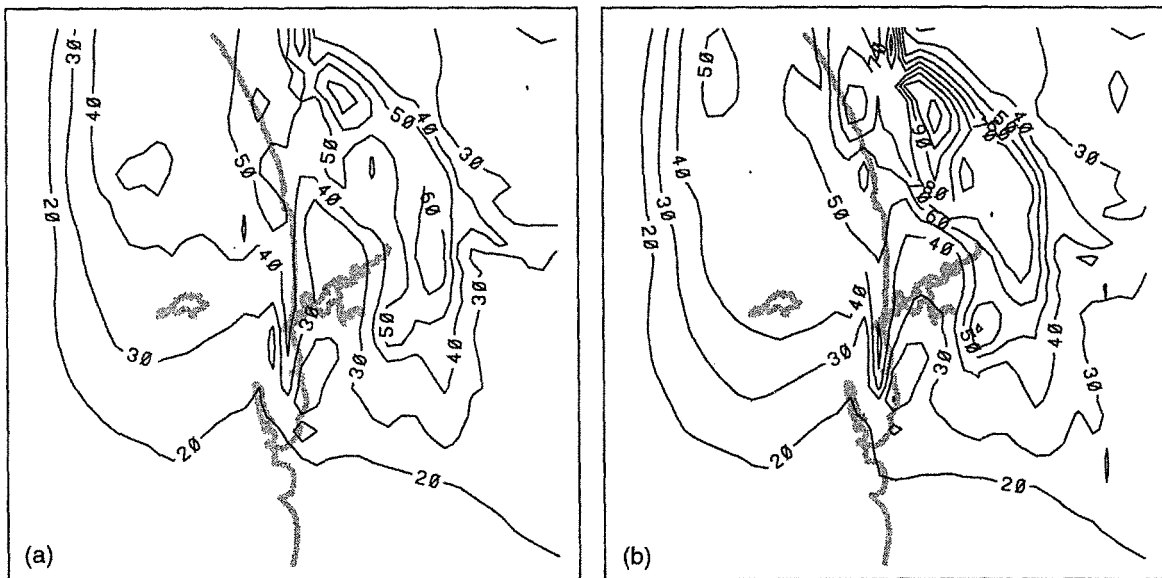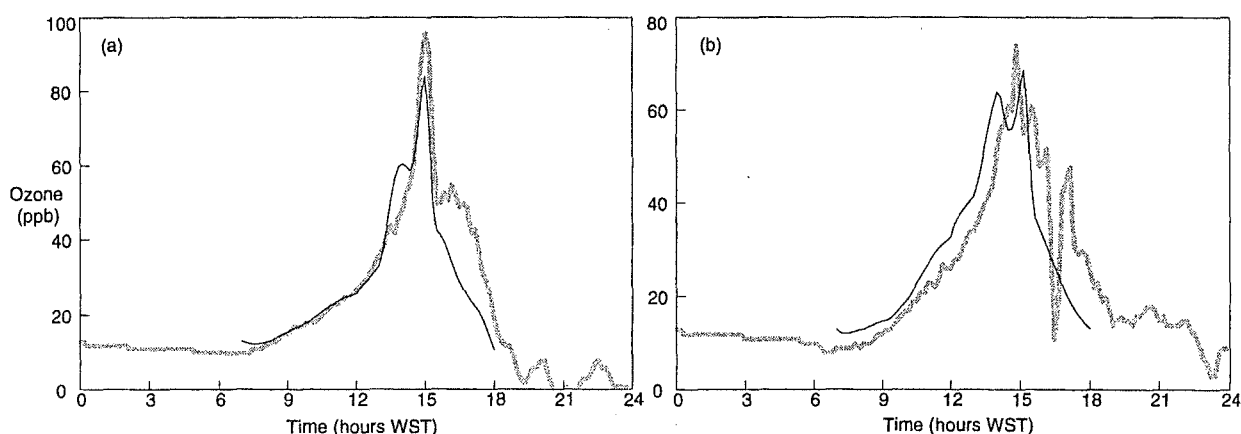

Figure 18. Modelled ozone concentrations for 3 p.m. on 16 March 1994. Case (a) is for emissions calculated in the standard inventory, with Kwinana ROC's tripled. Case (b) is for a model run with vehicle ROC emissions also increased 60%.

In Figure 18(b), the reduction is less, due to the increased reactivity of urban emissions, used for this run. Significant NO_x plumes are not generally seen at Cullacabardee (See Figure 1 for

location), more in keeping with Figure 18(b). This feature further supports the presumption of enhanced reactivity for urban emissions.

The effects of the increased ROC emissions on comparisons for Cullacabardee and Kenwick are shown in Figure 19. The quality of the validation was improved at Cullacabardee to a degree similar to that for Caversham, while that for Kenwick improved slightly. Checks of trends for modelled and measured SP_{max} and SP at Cullacabardee indicated the cause for the slight shortfall at Cullacabardee was an additional input of NO_x, in the modelled Kwinana plume. This NO_x was not found in the measured trace.

The end result from the 16 March analysis was the adoption of a standard adjustment factor of two, when processing vehicular emissions. The cause was presumed to be a shortcoming of the Carbon bond IV chemistry model, although this conclusion was not certain.

Figure 19. Comparisons of modelled (solid line) and measured (broad shaded line) ozone concentrations at Cullacabardee (a) and Kenwick (b), for 16 March 1994. For these cases, modelled ROC emissions were increased by 60%.

9.4. 18 March 1994

The smog event on this day was broadly similar to that on 16 March. However, the sea breeze front moved inland more slowly, and the measured ozone peaks were of longer duration.

Model simulations were only run for the daytime period (6 a.m. to 6 p.m.) because trajectory analyses showed that only daytime emissions contributed to the day's ozone concentrations.

With the slower inland movement of the sea breeze front, the potential contribution from Kwinana emissions was one of the greatest of all the days studied. This case was therefore a good one for analysis of model sensitivity changes in the Kwinana emissions inventory.

9.4.1. Data Used

For this day's modelling, measured meteorology was again used. This decision was based partly on the experience in modelling the 16 March event, and partly on the difficulty of obtaining a sufficiently close match to the slow inland progress of the sea breeze, in numerical modelling of the day's meteorology.

The data set available on the day was enhanced slightly by the availability of a temperature sounding from Perth Airport, at about 1 p.m.. A careful analysis of sodar records for mixing depth information was again used.

Based on previous experience, the base emissions inventory used in studying this day comprised NO_x as calculated, Kwinana ROC emissions tripled, urban vehicle ROC emissions doubled, plus half the calculated biogenic ROC emissions.

9.4.2. Model Results and Sensitivity Studies

Analysis of the model results for this day revealed a significant contrast to the results of 16 March. The modelling work for that day indicated general agreement across the inland sites only for a doubling of vehicle emissions, while that for 18 March showed good agreement for Caversham only, with generally low sensitivity to vehicular ROC emissions.

The reason for the lack of good validation for Cullacabardee and Kenwick appeared to be local wind direction fluctuations at these locations, which were not representative of the flow carrying the developing smog. These errors were particularly crucial on 18 March, because of the slow inland progress of the sea breeze. They meant that the modelled ozone peak arrived earlier than the actual peak at both sites.

The reason for good agreement at Caversham (Figure 20) appears to be the already-indicated good validation of NO_x estimates, in combination with indications of NOx-limited conditions from both measurements and modelling during the early afternoon. This was the case for both the standard vehicle emissions inventory, and for the doubled vehicular ROC case. The trend shown by the solid line in Figure 20 coincided almost exactly with that for the standard vehicle ROC emissions.

Also shown in Figure 20 is the consequence of an alternate emissions inventory, based on plume sampling conducted by the CSIRO during the 1994 intensive study period (Carras, Clark, Hacker, Nelson and Williams, 1995). This investigation was conducted to investigate effects of measured variations from the calculated inventory.

ROC emissions from Kwinana were dominated by a single source, which contributed 90% of the total. Table 2 shows emissions for this source, taken from the inventory. The averages of
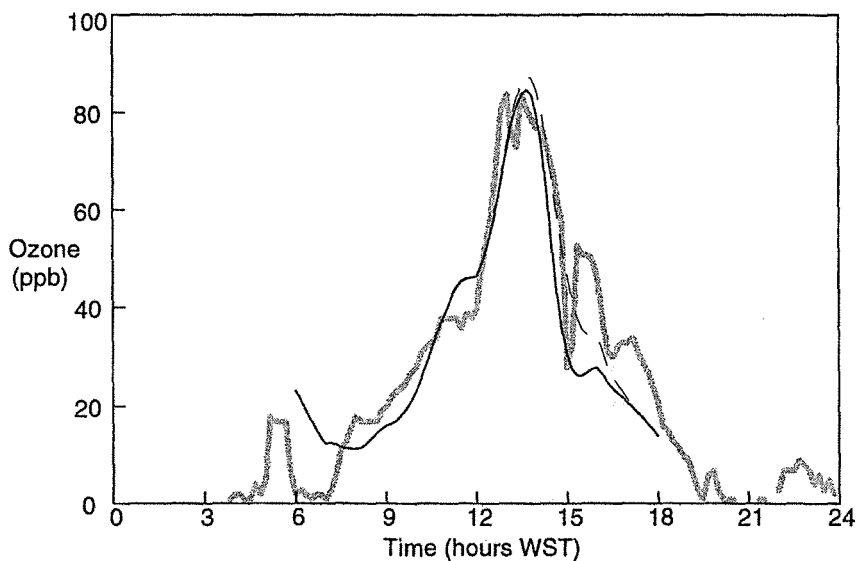
Figure 20. Measured (wide shaded line) ozone concentrations for Caversham compared with model results for the tripled-ROC Kwinana inventory (solid line), and for the inventory with revisions based on CSIRO measurements (broken line), for 18 March 1994.

29

	Inventory (kg/hr)	Ratio to ">C4 Alkanes"	Averaged CSIRO measurements 5 & 12 (ppbC)	Ratio to ">C4 Alkanes"	Revisions to inventory (kg/hr)
Ethane	110.858	0.1700			
Propane	360.807	0.5532	279.0	0.5981	
Butane	199.385	0.3057	156.2	0.3348	
>C4 alkanes	652.228	1.0000	466.5	1.0000	
Ethylene	0.000	0.0000	58.3	0.1250	77.7
Propene	32.061	0.0492	7.8	0.0167	10.4
1-Butene	2.712	0.0042			
2-Butene	0.000	0.0000			
>C4 alkenes	0.000	0.0000			
Isopropene	0.000	0.0000			
Acetylene	0.000	0.0000	4.8	0.0103	6.4
Benzene	7.018	0.0108	29.7	0.0637	39.6
Toluene	8.135	0.0125	100.1	0.2146	133.4
Xylene	3.509	0.0054			
Other Aromatics	55.509	0.0851			
Formaldehyde	162.858	0.2497			

Table 2. Calculations of revisions to Kwinana emissions, based CSIRO intensive study measurements. Inventory revisions were based on an assumption of 6 carbon atoms in >C4 alkanes.

CSIRO measurements 5 and 12, quoted in Table 16 of Carras et al., are also shown.

The CSIRO measurements are expressed in terms of parts per billion of carbon (ppbC), which is proportional to the mass density of carbon in the samples. Since carbon is the dominant mass component of ROC, the relative magnitudes of the CSIRO measurements should closely match the relative mass densities of ROC in the atmosphere. They therefore provide a measure of relative mass emission rates, which may be compared to inventory estimates.

The relativities are shown by the two "Ratio" columns in Table 2. The results show good consistency for most alkanes. However, ethylene, benzene, toluene and acetylene were measured in greater concentrations than would have been expected on the basis on the inventory, and less propene was present. To check the potential effect of these differences, some revisions to the inventory were made, based on the mass emission ratios implied by the CSIRO measurements (shown in the right-hand column of Table 2). The increased total mass emission was compensated by reducing the standard Kwinana ROC scaling factor of 3 to 2.6.

There was a significant sampling difference between measurements 5 and 12. The former was taken over a long time interval, in a tedlar bag, while the latter was a flask sample, so was essentially instantaneous. Sample 5 showed a high ethylene concentration, while sample 12 showed none. Given that one sample included ethylene, while the other did not, it is possible that the ethylene plume from Kwinana is of much narrower extent than the general mass of emissions. The source might be more localised, and possibly not from the main ROC source.

The effect of the altered emissions pattern on ozone concentrations in Figure 20 shows that Kwinana emissions mainly affected the latter part of the ozone peak, having a noticeable but secondary effect.

There is, however, one qualification which must be made about the result. The ethylene fraction of the plume was derived from the average of samples 5 and 12. Given the longer sampling time of sample 5, the high fraction measured in this sample might be more representative, doubling the potential ethylene contribution.

The source of the poor model validation at Cullacabardee for 18 March is supported by a comparison for a grid location further downwind. Figure 21 shows that at a site where the time of the modelled peak matched the time of the peak measured at Cullacabardee, there was much better agreement.
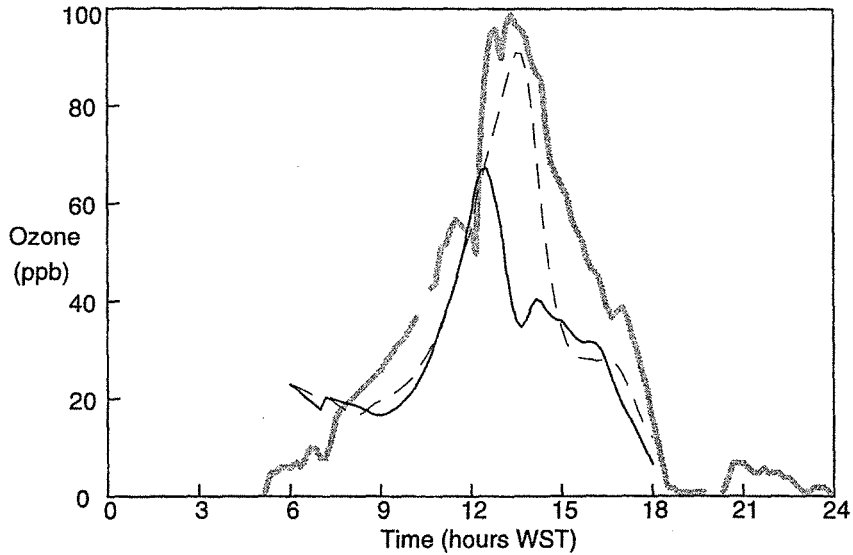
Figure 21. Measured (wide shaded line) ozone concentrations for Cullacabardee compared with model results at Cullacabardee (solid line), and for a location 6 km east and 6 km north (broken line), for 18 March 1994.
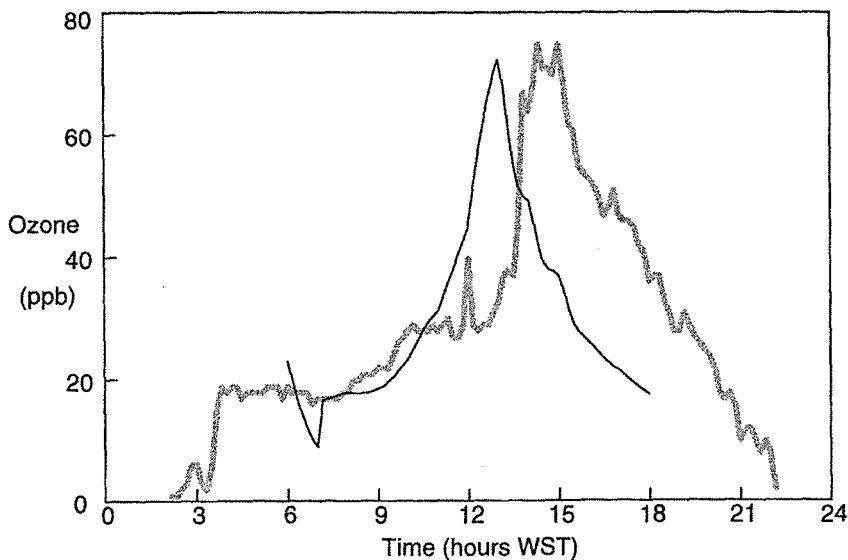
Figure 22. Measured (wide shaded line) ozone concentrations for Kenwick compared with model results (solid line), for 18 March 1994.

Also evident in figures 20 and 21 is a general low trend of ozone concentrations after the peaks. This is a general characteristic of model results for such events. Also typical of these periods is a close match of modelled and measured SP_{max}. The calculated air trajectories for these periods always pass through Kwinana, suggesting that the ozone error is an effect of a shortfall in modelled reactivity from the Kwinana region.

The comparison for Kenwick revealed a fair match of peak calculated ozone (Figure 22) and SP_{max} concentrations, but at different times for model and measurement. Both peaks corresponded to the time (based on modelled or measured windfields) when the back-trajectory to Kenwick passed through Kwinana.

Both ozone and SP_{max} concentrations were modelled slightly low, with a close match of the modelled plume reactivity.

9.5. 21 March 1994

The ozone event on this day had much in common with those on the 16 and 18 March. It was chosen for study on the basis that is lacked the high early winds of the 16 March, and the slowing of the sea breeze front of the 18 March. This made it a good basis for comparison of measured and modelled events, where the measured or modelled meteorology could be used for transport calculations.

9.5.1 Data Used

The meteorological model was run initially at a resolution of 12 km in the west-east direction, and 80 km in the south-north direction. On the morning of the third day of the model run, a sharp coastal trough had formed (Figure 23). The second, higher resolution run of the model used the third day's output files to provide initial and boundary conditions.
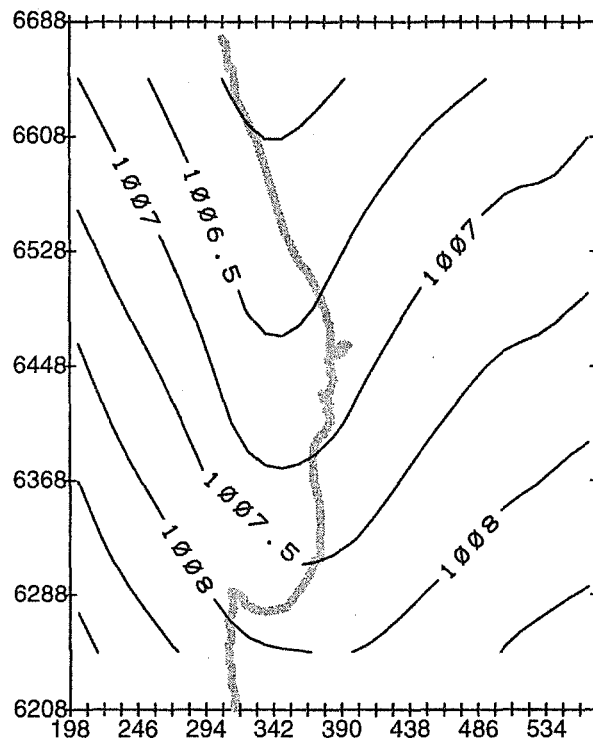
Figure 23. Air pressures (hPa) modelled near Perth for the morning of 21 March 1994. A coastal trough is clearly in evidence.

32

This run used resolutions of 6 by 10 km, covering a region 360 km from west to east, and 250 km from north to south. A rather larger west-to-east extent was found necessary for the effects of the trough to the west to be represented adequately.

In the low-resolution run the modelled trough progressed inland during the modelled day. However, it was always necessary to apply extra forcing in the higher-resolution run, to ensure the time and rate of passage of the sea breeze inland matched measurements. This was achived by applying a trend of pressure gradient. In the case for 21 March, the nominal gradient wind was changed from 14 kt from 60° to 40 kt from 210°. The actual pressure gradient change did not, however, match this trend, since internal divergences tended to develop and counteract the externally-applied change.

The model equations include a response to the surface pressure gradient at all levels. This meant that, when such a forcing term was applied, there was a trend toward south westerly winds at all levels. As a result of the model's horizontal temperature gradients, spurious cooling could occur in the levels immediately above the sea breeze. In the model, this effect could be numerically counteracted by applying a layer-by-layer artificial temperature trend.

In reality, the movement of the trough inland is driven by external trends involving changes both of larger-scale pressure gradients, and the temperatures of approaching air masses. The effects of such trends can be modelled, but they are normally not known in sufficient detail. While adjustments such as the above must be made, there are many possibilities for interference with the physics of the trough and the sea breeze. Care must therefore be taken in the choice of applied external trends.

However, with these changes applied, it is possible to produce a detailed three-dimensional picture of the inland wind and stability structure. Figure 24 shows an example, of potential temperature and mixing depth at the time of peak ozone concentrations on 21 March.

For model runs using measurements, meteorological data were obtained in a manner identical to the runs for 18 March (See section 9.4.2).

9.5.2 Model Results

Ozone time sequences for the Caversham site, modelled and measured, are shown in Figure 25. Estimates based on both modelled and measured meteorology are higher than measurements before sea breeze arrival, close to correct at the ozone peak, and slightly low afterward (the last, for reasons already discussed in section 9.4.2). There are, however, significant differences in the variation close to the time of peak concentration.

These appear to relate to greater inland mixing depths calculated by the numerical model. This permitted stronger vertical motions near the sea breeze front, particularly in the period from 13 to 14 hours WST. The resulting entrainment of clean air caused oscillations of ozone concentration either side of the peak, when numerical model calculations were used.

Figure 26 demonstrates the general nature of the difference. The narrowness of the peak in Figure 26(a), compared to Figure 26(b), is clearly evident, as is the narrow band of decreased concentration both inland and seaward of the band of highest concentration.

Also evident is a double maximum along the band of peak concentrations, most evident in Figure 26(b). The southern peak was due to morning emissions from Kwinana combined with some mid-day urban contribution, while the northern one was due to mid-day urban emissions. The ozone formed from morning urban emissions is evident in both Figure 26(a) and (b) as a pool of moderate ozone concentrations just offshore, near the northern boundary of the model grid.
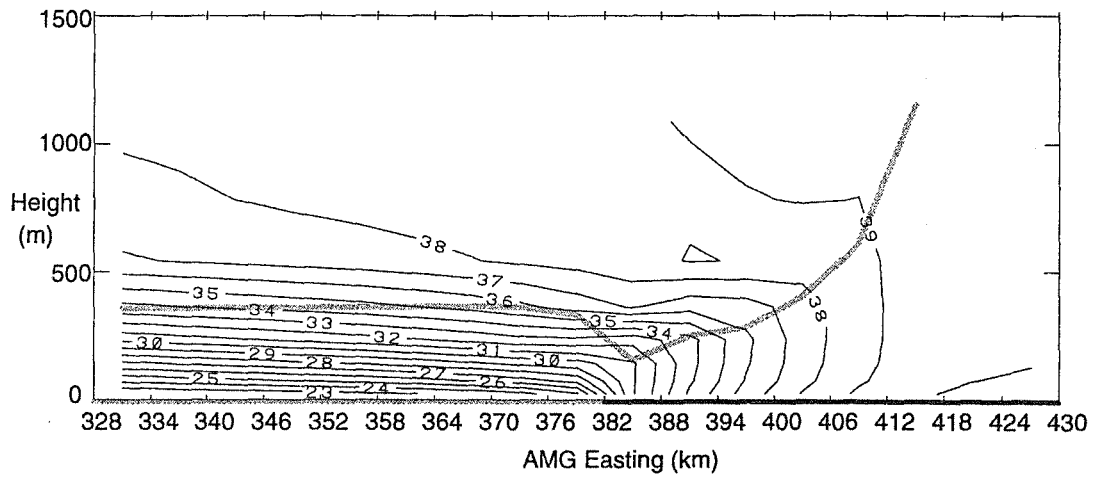
Figure 24. Potential temperature and mixing depth (shaded line) cross-section near Perth, modelled for 3 p.m. on 21 March 1994.
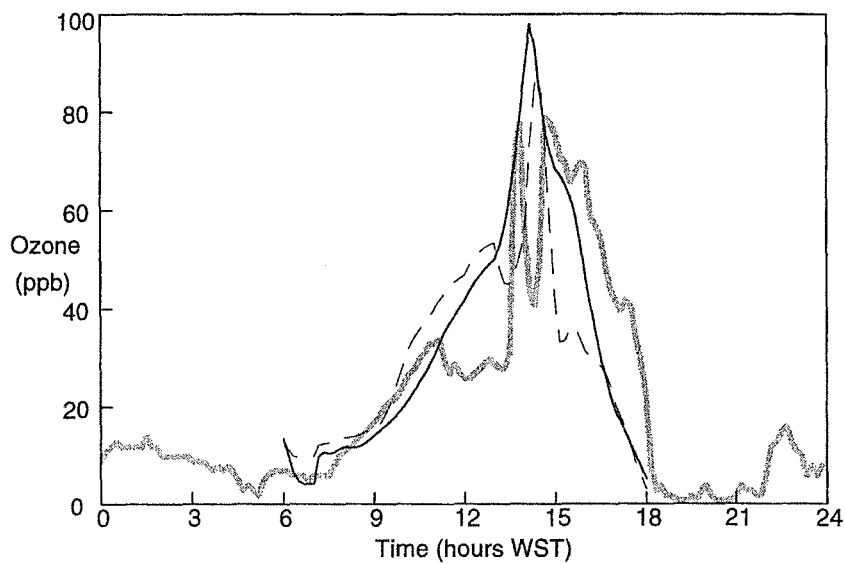
Figure 25. Ozone concentrations at Caversham for 21 March 1994. The broad shaded line represents measurements, the solid line model results using measured meteorology, and the dashed line model results using modelled meteorology.

34
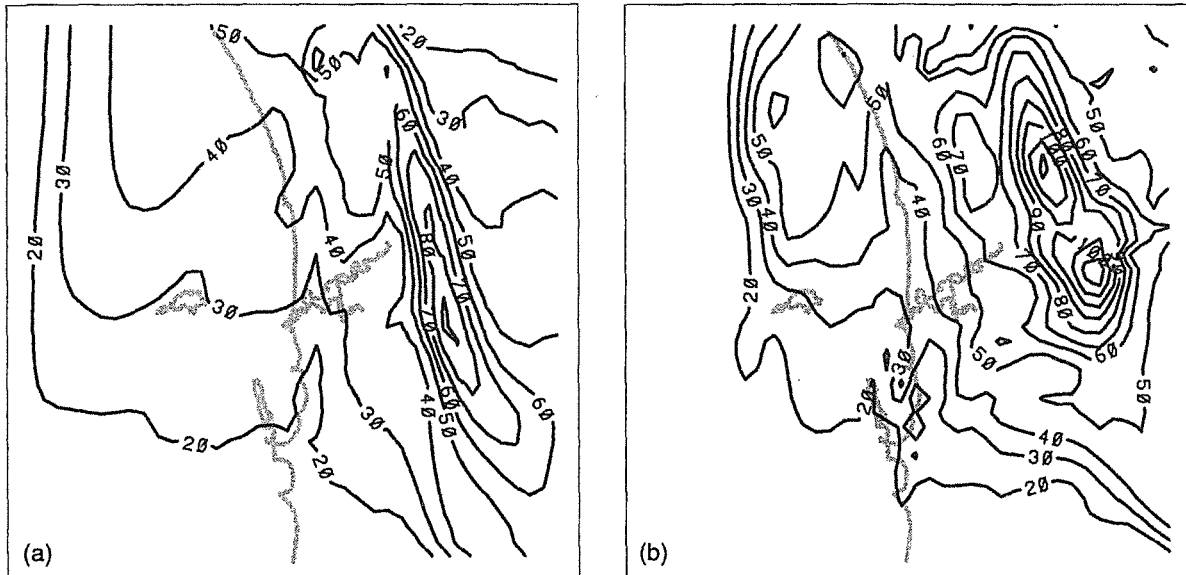
Figure 26. Ozone concentrations (ppb) calculated for 3 p.m. on 21 March 1994, using (a) modelled and (b) measured meteorology

9.6. 8 January 1993

This was the day when the highest ozone concentrations were measured inland, during the whole three years of the study. Conditions for the day were forecast to be cool, after the passage inland of the coastal trough. As a result, no radiosonde releases were scheduled.

However, the forecast proved inaccurate, with light offshore winds, and a light southwesterly developing mid-morning. High ozone levels were measured at all metropolitan sites. Trajectory analyses indicated that Caversham, Cullacabardee, Kenwick and Rolling Green received the morning's urban and Kwinana emissions, while ozone at Two Rocks and Quinns Rocks resulted from a combination of the previous evening's emissions from Kwinana, and overnight emissions from the metropolitan area. Trajectories to Swanbourne based on surface winds originated well to the south of Perth, and it is possible that high ozone levels there were due to some three-dimensional transport involving more easterly upper-level winds.

9.6.1 Data Used

While there was a lack of data for the day, the significance of the event in the study period resulted in a careful analysis of contributing conditions. Sodar wind profiles at Cullacabardee were analysed for shear layers, indicative of the mixing depth. Values before sunrise in the 150 to 200 metre range were discernible, but little useful data were available from this source in the crucial period from sunrise to noon.

However, the 6 a.m. radiosonde release from Perth Airport showed a strong stable layer to about 500 metres. From this temperature profile, and measured surface temperatures across the region, it was possible to construct a mixing depth field through the morning.

Few reliable measurements of mixing depth within the sea breeze inflow were available. Some mid-afternoon sodar profiles indicated a transition to return flow above 450 metres, and the 6 p.m. Perth Airport radiosonde showed a clear inversion base at 400 metres.

Mixing depths after sunset were of no significance to daytime ozone levels, a fortunate fact since there was little information available from sodar profiles. However, the decay of the sea

35

breeze would have permitted mixing depths to decrease, so a general trend down to 200 metres at midnight was presumed.

Wind measurements were more readily available. The Cullacabardee sodar, and wind profiles measured using Perth Airport balloon releases at 6 a.m., noon and 6 p.m., provided general windfields, and the extensive surface monitoring network recorded well the passage of the sea breeze.

The emissions data used took account of experience with the 18 March 1994 analysis. Kwinana ROC emissions were increased by a factor of three, and vehicular ROCs by a factor of two.

9.6.2. Model Results and Sensitivity Studies

With the above mixing depth and wind data, useful accuracy was obtained from the very first run of the model (e.g., Figure 27). Both ozone and SP_{max} values were in fair agreement with measurement. The major difference was a shorter duration of the modelled peaks, and correspondingly higher concentrations. These discrepancies compensated when hourly averages were analysed (as in Figure 28), suggesting that the modelled peaks suffered less lateral dispersion than the actual ones.

Subsequent experiments, with small changes to mixing depths and surface wind data sets altered the quality of the validation little.

The first of these changes arose from an observation that, of the three inland sites, only the ozone concentrations at Cullacabardee were notably above measurements. Morning surface temperatures were seen to be higher at,this site than at Caversham and Kenwick. Inclusion of a north-to-south mixing depth trend, based on site-by-site surface temperatures and the Perth Airport morning temperature profile, rectified most of the difference.

The potential effect of the lack of wind data between the coast and Rottnest Island was also studied. An artificial wind measurement, located 12 km offshore, of 2 m s^{-1} from 180°,
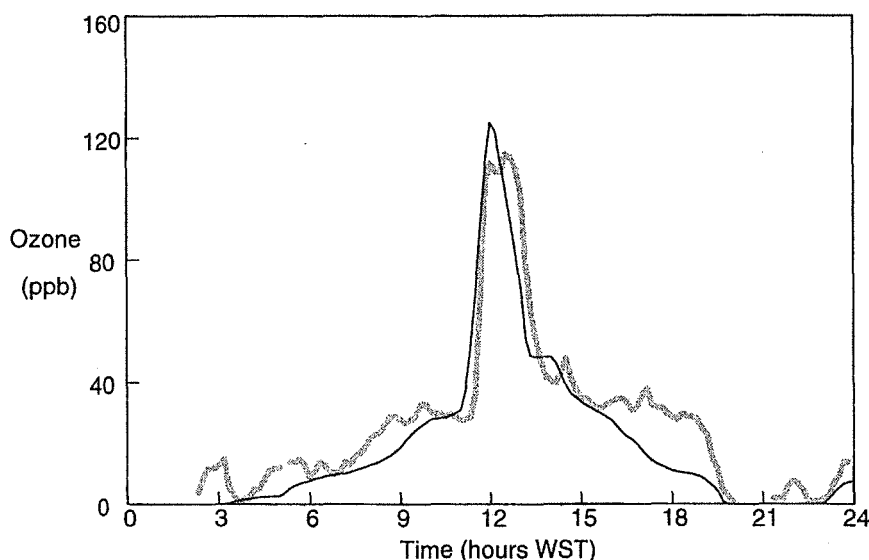
Figure 27. Instananeous ozone concentrations at Caversham for 8 January 1993. The broad shaded line represents measurements, the solid line model results.

36
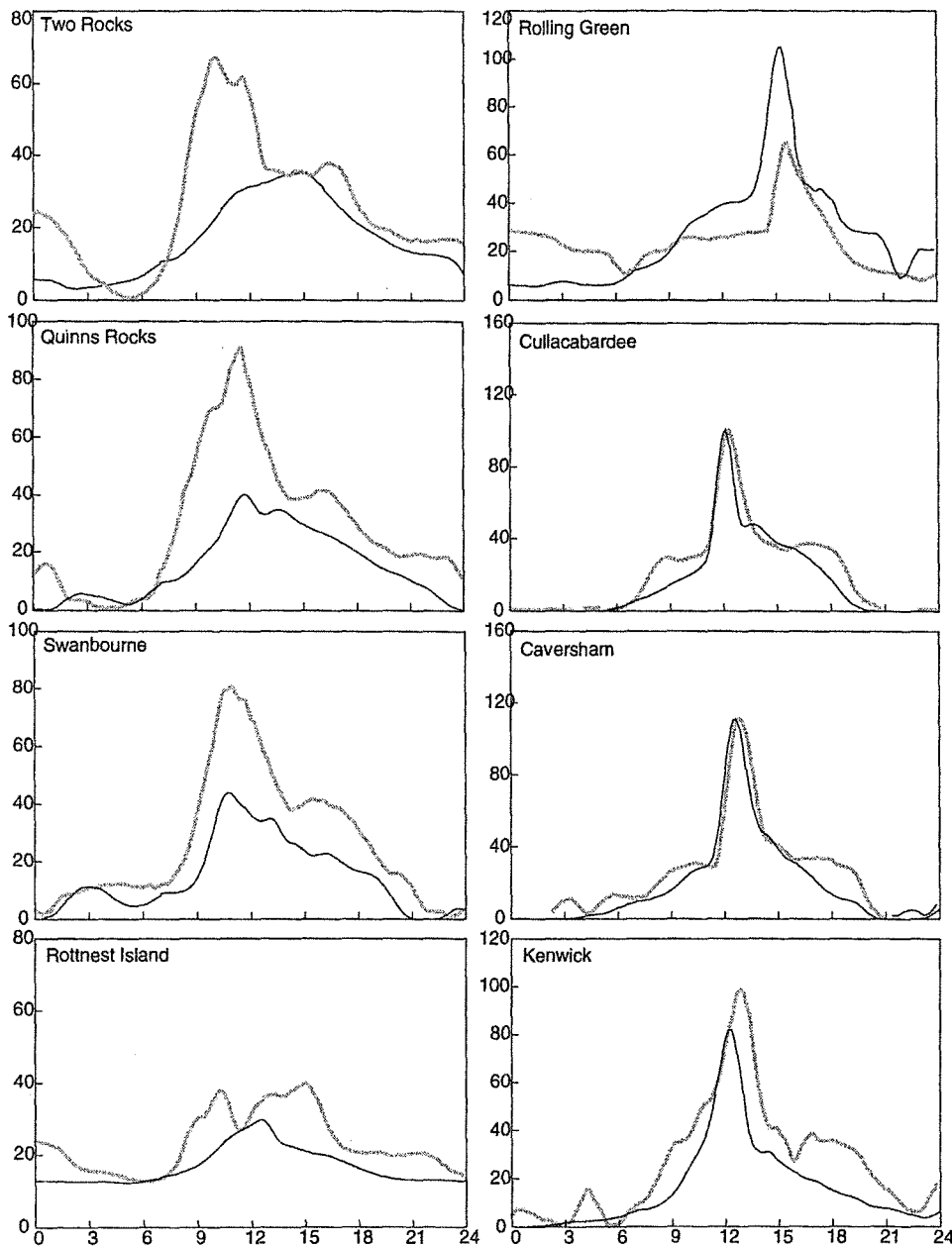
Figure 28. Time sequences of hourly average ozone concentrations (ppb) at all operational sites within the PPSS region, on 8 January 1993. The broad shaded lines represent measurements, the thin black lines model calulcations.

between 6 a.m. to 10 a.m., was added to the data set. This redirected the trajectory leaving Kwinana at 5 a.m. exactly over the Caversham site at noon, so maximising the potential impact of Kwinana emissions there. There was, however, little effect on modelled ozone concentrations at Caversham.

While inland metropolitan concentrations were well handled, modelled ozone concentrations at other sites were in poorer agreement (Figure 28). Those at Rolling Green were well in excess of measurements, probably due to the lack of inland mixing depth data. This result indicates that the modelled fields for this day should not be used to infer inland ozone trends.

37

In contrast, ozone concentrations at coastal sites were significantly underestimated. This may reflect two effects,

1. the uncertainties of the meteorology of the overnight period, when the emissions contributing to smog at these sites were released, and

2. smog residing in the coastal trough, from transport offshore of the previous day's urban emissions

Calculations from a model run for the previous day were used to initialise the 8 January run, but these had little effect on calculated concentrations. On the basis of the initial distribution of smog species, modelled by the preceding day's run, and this result, it was felt that the first of the above possibilities was the more likely.

Although good validation was obtained only for inland sites, the quality of the validation at these locations made the event a useful one for sensitivity analyses. In particular, since there were indications that the air bearing the main smog mass had passed over Kwinana, the role of Kwinana emissions was again reviewed.

In this exercise, comparison model runs were made with all Kwinana emissions set to zero, then with only NO_x emissions zeroed. The former resulted in no significant alteration to peak ozone levels at Caversham and Cullacabardee, and a 10% decrease at Kenwick. The latter increased the peak by a few percent at these sites. These indicated that Kwinana emissions had only a minor effect on inland ozone levels on this day.

Model results for this day were also used to test the importance of biogenic emissions. These were set to zero, resulting in a decrease of ozone peaks at Caversham and Cullacabardee from about 110 ppb to 90 ppb.

Figure 29 shows the distribution of modelled maximum hourly average concentrations. The peak, of 154 ppb, was located north of Caversham, in a region where some confidence in the accuracy of the model could be held. Due to the mixing depth uncertainties aleady noted, the secondary peak to its east is likely to be in error.
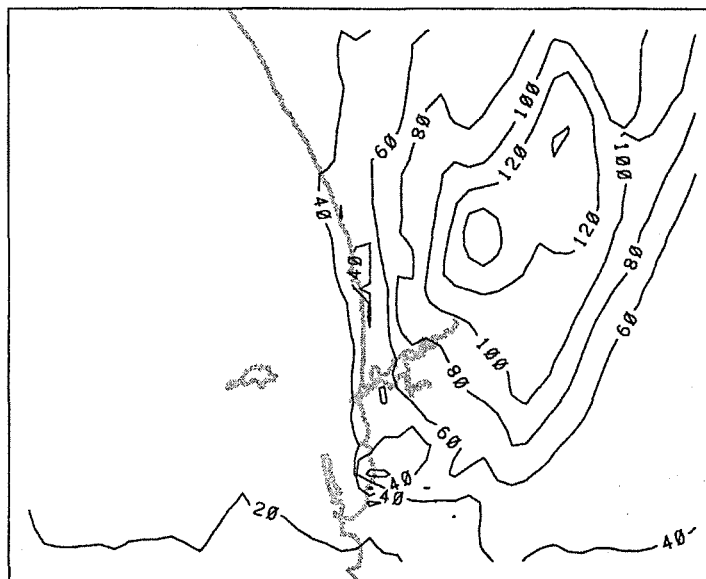
Figure 29. Maximum hourly average ozone concentrations modelled using UAM, for 8 January 1993.

9.7. 13 January 1993

This was a day on which ozone concentrations were primarily due to the reactivity of bushfire smoke. The meteorology of the day was relatively simple, with a persisting southerly to south westerly wind. The main uncertainty in the data used was a lack of knowledge of the concentration, or speciation, of incoming ROCs.

However, it was possible to match the reactivity of the incoming air mass to measurements, by adjusting the inflow concentrations until the trends of ozone, SP_{max} (and so reaction extents) matched. The estimate then allowed the future trend of ozone due to bushfire smoke, and the relative role of urban and smoke ROCs, to be estimated.

9.7.1. Data Used

Vertical temperature profiles were available only from the Perth Airport morning and evening radiosonde releases. However, these revealed similar upper-level potential temperatures (Figure 30). Maximum surface temperatures were about 29°C, showing that mixing depth remained limited at 500 to 600 metres all day. The profiles, along with measured surface temperatures, were used to create a record of general mixing depths used in the model.

The evening profile also showed a potential temperature of 31°C at 500 metres, consistent with an inflow lapse rate of about 0.02°C m^{-1}. In the conditions prevalent, the statistically-derived inflow stability estimates (See section 6.2.3) were inaccurate, so this value was used to provide TIBL growth estimates near the coast.

Detailed vertical wind profiles were only available from the Cullacabardee sodar, which suffered a failure at 3 p.m.. Fortunately, this was well after peak ozone concentrations had occurred, and an arbitrary vertical wind profile, of 7 m s^{-1} from 230°, was used to extend the
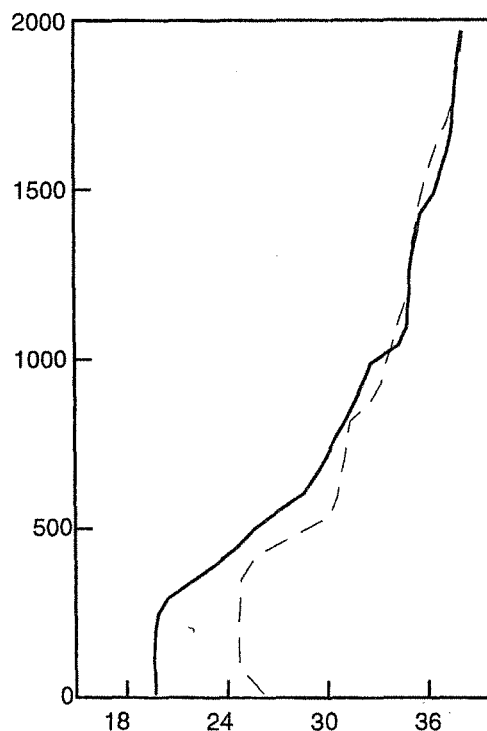
Figure 30. Vertical profiles of potential temperature measured at Perth Airport, at 6 a.m. (solid line) and 6 p.m. (dashed line) on 13 January 1993.

record to midnight.

The model run used the normal emissions inventory (with Kwinana ROCs tripled and vehicular ROCs doubled), the influence of smoke being imposed through modifications to initial and boundary conditions. The UAM species ethylene, olefins, paraffins, toluene and xylene were routinely parameterised as fractions of a "RHC" (reactive hydrocarbon) parameter, normally set to 0.018 ppm. The minimum value which gave ozone and SP_{max} concentrations in fair agreement with measurements at Cullacabardee and Caversham was found to be 500 ppb.

For reference, increased B_{sp} values within the Perth region occurred over the period 5 a.m. to 3 p.m., with a broad maximum over the time range 8 a.m. to 1 p.m.. At Hope Valley and Caversham, values over the latter time range were from 2 to 3 x 10^{-4} m^{-1}. At Queens Buildings, the range was from 3 to 4 x 10^{-4} m^{-1}.

The model initialisation used constant boundary conditions, replicating a flow of bushfire smoke uniform in time and space. However, because the peak smoke concentrations (as indicated by the B_{sp} values) covered the period from the start of the morning traffic peak, to the end of peak measured ozone concentrations, the excess modelled time period for the smoke was not an issue. The effects of spatial non-uniformity were explicitly considered, and are discussed in section 9.7.2.

9.7.2. Model Results

Comparisons between modelled and measured peak hourly average ozone concentrations, for measurement sites downwind of NO_x sources, were as follows:

Cullacabardee: modelled 64 ppb, measured 71 ppb. SP_{max} values were in better agreement, suggesting that the reactivity of the actual smoke plume may have been higher than modelled in the northern part of the region.

Caversham: modelled 95 ppb, measured 85 ppb. SP_{max} values were also about 10% high, indicating the modelled reactivity was close to correct.

Kenwick: modelled 63 ppb, measured 62 ppb, but the modelled peak was of much shorter duration. Modelled SP_{max} values were about 2/3 of measurements, indicating that the reactivity of the actual smoke mass was less, and actual NO_x values were higher.

Rolling Green: modelled 88 ppb, measured 111 ppb. Modelled and measured reaction extents were both one, so SP_{max} comparisons were equivalent. There was a peak ozone concentration of 141 ppb to the north (Figure 31), so the difference might simply reflect the lack of upper-wind data inland. (Surface winds at Rolling Green were 10 to $20°$ more northerly than close to the coast, but upper wind measurements made at Cullacabardee were the only ones available)

Ozone concentrations at Rolling Green before the peak were modelled low, but back trajectories indicated that the source of these was the previous evening's urban emissions. The model run commenced at midnight, so these were not included.

Peak modelled hourly-average ozone concentrations are shown in Figure 31. The overall pattern, with low concentrations at the coast, rising to a peak inland from the metropolitan area, appears typical of such events during the period of PPSS.

Overall, given the potential for significant variations of reactivity in the smoke plume across the metropolitan area, the validation was close to as good as could be expected. The event therefore provided a basis for study of the trends of ozone concentrations, to be expected in coming years.
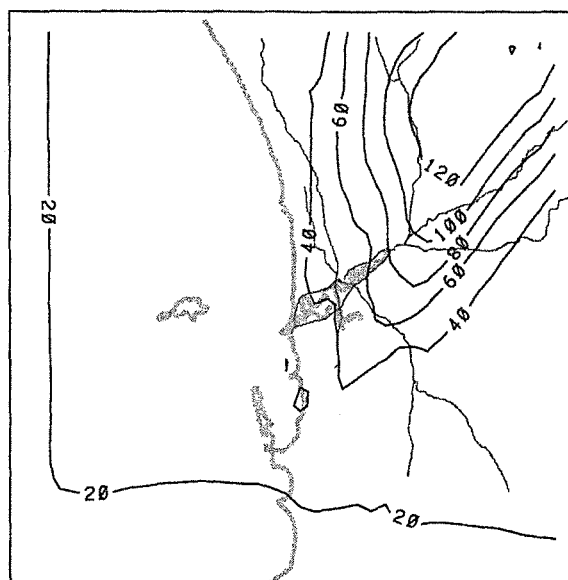
Figure 31. Peak hourly-averaged ozone concentrations, modelled for the smog event caused by bushfire smoke of 13 January 1993, using the lower RHC value of 500 ppb. The small contours in the top right of the figure correspond to 140 ppb.

As a first step in this analysis, the sensitivity of the validation to variations in RHC was checked. This was a significant issue, because modelling suggested greater reactivities in the northern suburbs, and Queens Buildings (on the northernmost of the three trajectories passing through the three haze monitoring sites) showed highest B_{sp} measurements.

It was found that a concentration of 750 ppb gave better validation at Cullacabardee, although Caversham estimates were then too high. The range from 500 to 750 ppb was therefore used to determine the level of uncertainty in estimation of potential trends.

Figure 32(a) and 32(b) show the estimated effects on peak ozone concentrations, for both 500 and 750 ppb RHC, of the change of emissions patterns from 1991 to 2011. Most evident in both plots is a general reduction in the north east metropolitan area, apparently due to the increased emissions of nitric oxide. However, inland, where smog reactions have had time to proceed, there are significant increases.

The 13 January 1993 was a day of moderate to fresh south westerly winds. More often in summer, morning winds are lighter. There is potential for the ozone increase to occur within the metropolitan area, on days when lighter winds ensure the smoke mass is not removed from the region so quickly.

Some features of Figure 32 require comment. Firstly, the higher reactivity present in case (b) has meant smaller decreases in peak ozone concentrations in the metropolitan area, and larger increases inland. However, in both cases there is a benefit to urban air quality, due to increased NO_x emissions, and a similar disbenefit to areas further inland.

From the shape of the region of ozone reduction, it might be taken that the source of the concentration change is emissions from the Kwinana industrial area. However, while Kwinana emissions were the dominant contributor in the southern metropolitan area, increased vehicle NO_x emissions were the major factor in the region of highest decrease, at its northern end.
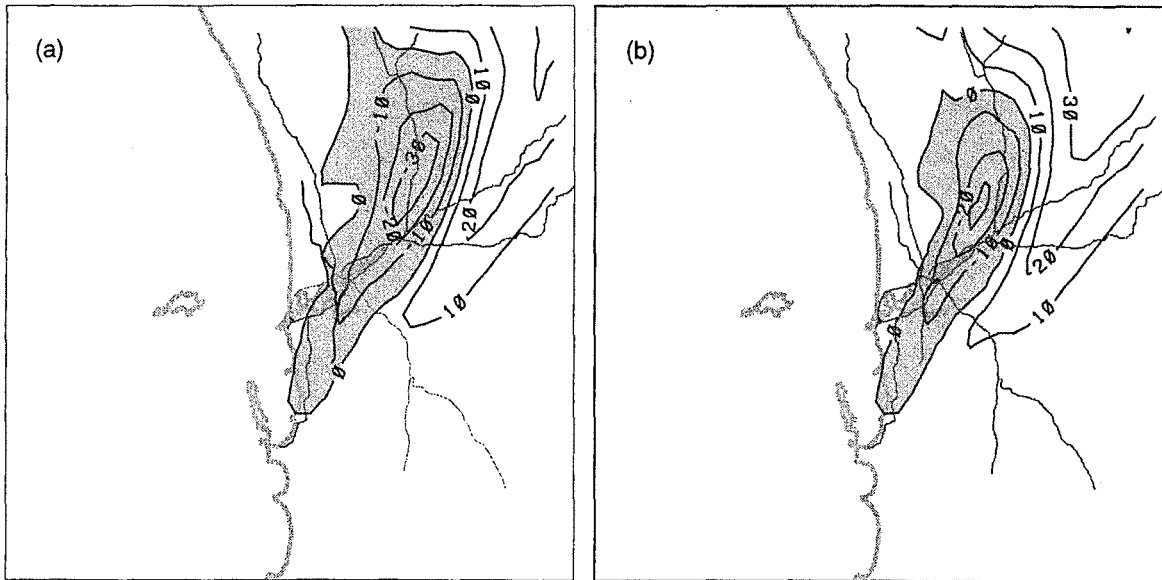
*Figure 32. Modelled changes to peak hourly average ozone concentration (ppb)
from 1991 to 2011, for the meteorology of the bushfire smoke event of 13
January 1993. Case (a) is for an incoming RHC concentration of 500 ppb, and
case (b) is for a concentration of 750 ppb. In the regions west and south
(upwind) of the contours, changes are uniformly zero*

10. Discussion

The most significant issue arising from evaluation of UAM is the apparent shortfall in the reactivity of urban emissions. Investigation of the implications revealed other problems, as yet unresolved, which may be related to this issue.

The emissions configuration used by the program was readily revised to match the year of interest. The area emissions inventory was based on population distribution, and maps of population estimates for 1992 and 2002 were provided. By interpolation and extrapolation (beyond 2002), an area emissions inventory for any year could be developed. The trend of total population was also used to adjust the industrial emissions totals. The vehicle emissions inventory included explicit inventories for 1986, 1991, 1996, 2001 and 2011, allowing interpolation to any year in the range provided.

Ozone and SP_{max} concentrations calculated at Caversham using this approach, for days matching the meteorology of 18 March 1994 are presented in figures 33 and 34. A downward trend is evident in the ozone plot, and a small upward trend in the SP_{max} plot. However, changes evident in the plots may include spurious effects, enhancing the apparent trend.

The downward ozone trend has arisen, in the model, from the effect of decreasing vehicular ROC emissions. However, the mass ratio of ROC to NO_x emissions in the vehicle inventory changed from 1.359 to 0.493 over period from 1991 to 2011 (James, 1995). There are already indications that Perth conditions are in the regime of known weakness of the Carbon Bond IV chemistry model used by UAM. For a downward change of this magnitude, there is a possibility that the benefits of the ROC decrease have been overestimated.

Figure 34 includes an unusual feature which may be associated with the ozone decrease. Over the period, total vehicular NO_x emissions were estimated to increase by a factor of 1.878. This change was closely matched by modeled NO_x concentrations, when NO_x emissions only were inserted into the model (Figure 35). However, the calculated SP_{max} values over the period from 11 a.m. to about 2 p.m, in Figure 34, fell from 1991 to 2001, before rising.
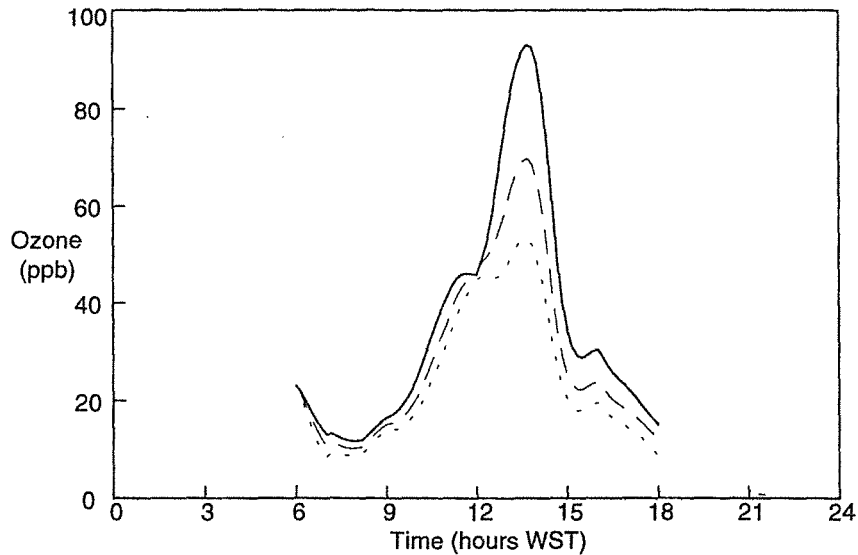
Figure 33. Ozone concentrations modelled for Caversham using measured meteorology for 18 March 1994, and emissions for 1991 (solid line), 2001 (dashed line) and 2011 (dotted line).The decrease appears to be spurious, and may be due to limitations of the model's chemistry scheme.
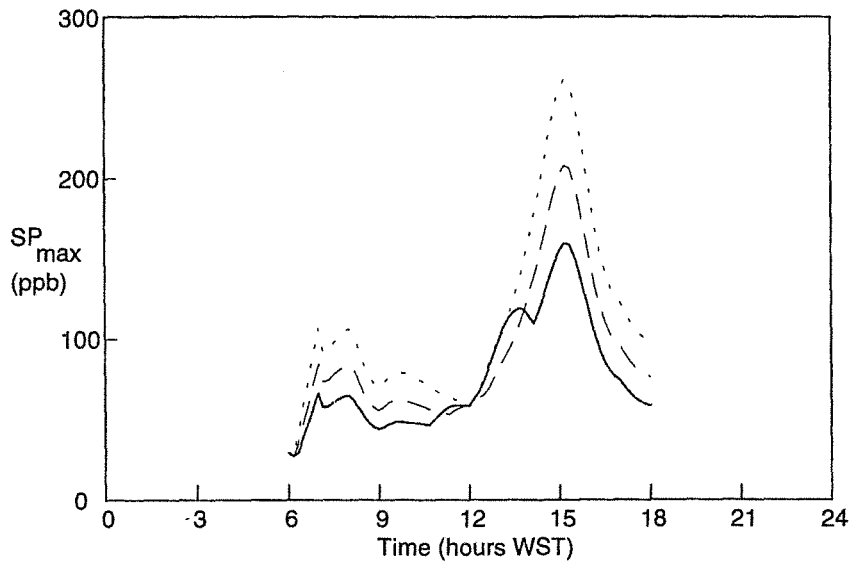
Figure 34. SP_{max} concentrations modelled using measured meteorology for 18 March 1994, and emissions for 1991 (solid line), 2001 (dashed line) and 2011 (dotted line). The absence of significant increases in the time range just after 12 noon is anomalous.
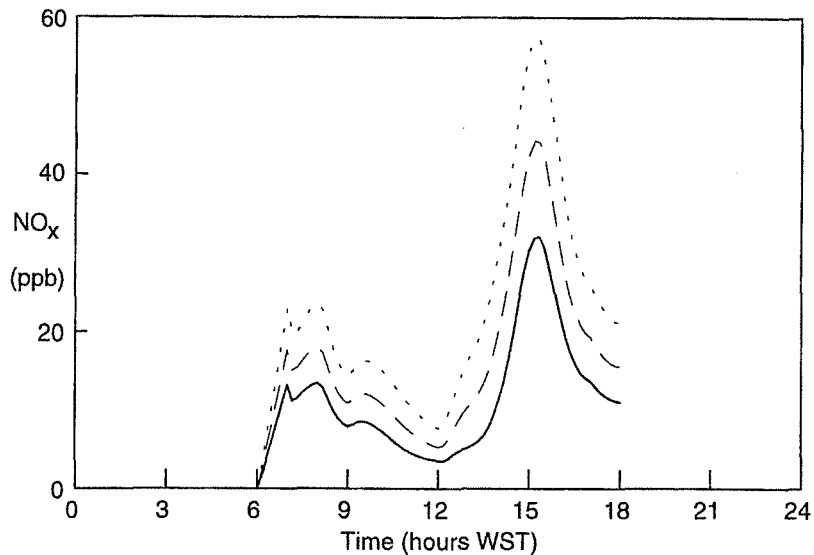
Figure 35. Calculated NO_x concentrations, using the meteorology of 18 March 1994, for model runs in which only NO_x was emitted. The case for 1991 emissions is shown by the solid line, for 2001 by the dashed line and for 2011 by the dotted line. The increase through this period matches the changes in the emissions inventory.

This result may indicate that the "SP_{max}" concept loses validity as the emission mix changes. Alternately, it may correspond to an error in the Carbon Bond IV mechanism. Both the Carbon Bond IV and IER chemistry models are known to have limitations, and as a result it is unclear whether the estimated trends are valid.

Also evident in all the days modelled so far is a low influence from Kwinana emissions, in the metropolitan area. However, there was an apparent contribution to moderate levels of smog modelled south of Kwinana, for 19 February 1994. There was also a potential contribution to coastal ozone concentrations on 8 January 1993, where model validation was poor.

For the modelled case of 18 March 1994, the magnitude and duration of high ozone concentrations was affected only slightly by inclusion of Kwinana emissions, and the duration of the peak was sensitive to potential errors in the inventory estimates. This day was characterised by a slow-moving sea breeze front, and wind directions were therefore more southerly, earlier in the afternoon. These conditions are those for which the greatest Kwinana influence could be expected.

Also evident on most days was a shortfall in calculated ozone concentrations late in the afternoon, although the SP_{max} estimator was usually close to correct. This implies a shortfall in modelled reactivity of the air passing inland, at a time when Kwinana emissions could be expected to have most influence. However, it is relevant to note that this error occurs well after the time of peak ozone concentration.

Overall, there are indications of either a significant error in the handling of the mix of emissions from Kwinana by the UAM model's chemistry scheme, or a major shortfall in reactivity of the inventory emissions - even when increased by a factor of three. A potentially relevant point is the absence of any temperature dependence of inventory ROC emissions estimates, although they are known to be heavily affected by temperature fluctutations in storage tanks. This would have greatest effect for mid-day emissions, which arrived at inland sites in the afternoon.

11. Conclusions and Recommendations

The Urban Airshed Model has proved useful in the development of photochemical airshed modelling at the W.A. DEP. However, there remain significant impediments to its confident application for air quality management in Perth, detailed below in sections 11.1 to 11.3.

11.1. Model Accuracy

In coastal smog events, and other events where smog reactions reached their full extent prior to passing a measurement site, the model performed well. However, there was a tendency to underestimate the extent of smog reactions when the initial, unmodified, emissions inventory was used.

Part of the discrepancy appears to be a shortfall in the estimates of fugitive ROC emissions from Kwinana industry. However, in view of the dominant role of urban ROC emissions, for which inventory estimates were supported by field measurements, other errors in the model appear to be more significant (See section 11.2).

11.2. ROC Emissions

Discrepancies in the reactivity of urban emissions, calculated by the program, are consistent with an error in the vehicle emissions inventory, in total emitted reactive organic compounds (ROC), of close to a factor of two. This error could have four causes:

- an actual underestimation of ROC emissions in the inventory. However, validation studies do not support this as a conclusion.

- emissions comprising more reactive species, compared to the normal mix presumed in inventory development. Given the high temperatures of Perth smog days, and the high volatility of the lighter and more reactive chemical species in petrol, this is a feasible contributor to the observed effect. However, experimental evidence does not support this possibility.

- shortcomings in the chemistry model employed within UAM. The scheme used has known limitations, but no record of model performance in conditions close to those of Perth has yet been found.

- an equivalent mass emission error in the area sources inventory. This appears unlikely, because of the relatively smaller total emissions from these sources.

If the error is attributed to limitations of the chemistry model, a decrease of ROC emissions would take the conditions further into its regime of weakness, giving an enhanced decrease of ozone concentrations. This means that, if UAM is used for air quality planning in Perth, any effect of changes to vehicle ROC emissions may be overestimated.

Initial studies of predicted trends in ozone concentrations to the year 2011 have shown results consistent with this conclusion.

To the extent that reactivity errors found in modelling matched qualitatively those found in smog chamber experiments, the estimated vehicular emissions of volatile organic compounds (ROC) have received some support from modelling.

Several problems in representing the effect of ROC emissions by Kwinana industry were highlighted, and the relative significance of model limitations and inventory shortcomings is

not yet finally resolved.[1] Although a relatively small contribution to smog events in the metropolitan area was found, the actual size of the contribution remains uncertain.

11.3. NO_x Emissions

At no point did modelling suggest that the PPSS inventory of emissions of nitrogen oxides (NO_x) was in error. Values of the IER parameter SP_{max}, which is indicative of the combined accuracy of meteorology and NO_x emissions, were usually in good agreement with measurement.

There were indications that the concentrations of nitrogen oxides reaching the metropolitan area, from Kwinana, were modelled too high. This may have been due to an error in modelled reactivity of ROC emissions, rather than an error in NO_x emissions estimates.

11.4. Modelling Issues

Modelled SP_{max} values were found, in sensitivity studies, to be largely independent of emissions of ROC. This supports the applicability of the IER analysis model, and by inference the Generic Reaction Set reaction model, to the Perth metropolitan area.

The computation grid used in UAM, with fixed numbers of layers below and above the mixing depth, resulted in low sensitivity of calculated concentrations to vertical resolution. It is therefore a significant contributor to the speed of execution of the model.

The meteorological monitoring maintained during the study was of sufficient extent and accuracy to permit direct use of measurements to construct the meteorological data required by the model. This result differs from experience elsewhere in Australia. It reflects both the simplicity of the meteorological fields on the Perth coastal plain, due to the relative straight coastline, and also good design of the monitoring network.

The success of modelling using measurements means that difficulties in obtaining good wind and temperature fields from numerical models are of minor concern, but also suggests that there is a continuing need for meteorological monitoring, particularly close to the line between Rottnest Island and Rolling Green.

12. Acknowledgements

The assistance of Martin Cope, of the Victorian Environment Protection Authority, in providing advice at many stages of the use of UAM, particularly in the implementation of the emissions inventory, is gratefully acknowledged.

The direct contribution of DEP monitoring staff, in maintaining a high standard of air quality and meteorological measurements through the whole period of the study, was also crucial to the success of this work.

13. References

Azzi, M., Johnson, G.J. and Cope, M., 1992, "An Introduction to the Generic Reaction Set Photochemical Smog Mechanism", Proc. 11th Intern. Clean Air Conf., Brisbane, 5-10 July, p. 451-462.

---

[1] Subsequent to the completion of this report, and of PPSS, emissions estimates were revised by BP, and now match closely the meaurements made during PPSS.

Beard, J.S., 1979a, "Vegetation Survey of Western Australia. The Vegetation of the Perth Area", Vegmap Publications, 6 Fraser Road, Applecross, Western Australia 6153.

Beard, J.S., 1979b, "Vegetation Survey of Western Australia. The Vegetation of the Pinjarra Area", Vegmap Publications, 6 Fraser Road, Applecross, Western Australia 6153.

Brost, R.A. and J.C. Wyngaard 1978, "A model study of the stably stratified planetary boundary layer", J. Atmos. Sci. **35**, 1427-1440.

Carnovale, F., Alviano, P., Carvalho, C., Deitch, G., Jiang, S., Macaulay, D., and Summers, M., 1991, "Air Emissions Inventory Port Phillip Control Region: Planning for the Future", Environment Protection Authority of Victoria, December 1991.

Carras, J.N., Clark, N.J., Hacker, J.M., Nelson, P.F. and Williams, D.J., "Airborne Measurements of Urban and Industrial Plumes in the Perth Region, Summer 1994". Flinders Institute of Atmospheric and Marine Sciences, Flinders University, South Australia.

Deardorff, J.W., 1980. "Laboratory study of entrainment rate in a convectively mixed layer", Third Conference on Ocean-Atmosphere Interaction, Jan 30 - Feb. 1, Los Angeles, Calif.

Gonzalez, R.C. and Wintz, P., 1987, "Digital Image Processing", Addison-Wesley, Mass.

Goodin, W.R., McRae, G.J. and Seinfeld, J.H., 1979, "A Comparison of Interpolation Models for Sparse Data: Application to Wind and Concentration Fields", Jour. Appl. Meteor. **18**, p. 761-771.

Guenther, A., Zimmerman, P. and Wildermuth, M., 1994, "Natural Volatile Organic Compound Emission Rate Estimates for U.S. Woodland Landscapes", Atmos. Environ. *28*, p 1197-1210.

Hess, G.D., B.B. Hicks and T. Yamada, 1981, "The impact of the Wangara experiment", Bound. Layer Met. **20**, 135-174.

Hingston, F.J., Dimmock, G.M. and Turton, A.G., 1980, "Nutrient Distribution in a Jarrah (*Eucalyptus Marginata* Donn ex Sm) Ecosystem in South-West Western Australia", Forest Ecol. Manag. *3*, p 183-207.

James, B., 1995, "Motor Vehicle Emissions Inventory for the Perth Photochemical Smog Study", Department of Transport.

Johnson, G.M., 1984. "A Simple Model for Predicting the Ozone Concentration of Ambient Air", *Proc. Eighth Intern. Clean Air Conf., Melbourne, 6-11 May 1984*, 2, 715-731.

Killus, J.P., Myer, J.P., Durran, D.R., Anderson, G.E., Jerskey, T.N., Reynolds, S.D. and Ames, J., 1984, "Continued Research in Air Pollution Simulation Modeling, Vol. V: Refinements in Numerical analysis, Transport, Chemistry, and Pollutant Removal", EPA-600/4-76-016c, U.S. Environmental Protection Agency, Research Triangle Park, North Carolina.

Lamb, B., Gay, D. and Westberg, H., 1993, "A Biogenic Hydrocarbon Emission Inventory for the U.S.A. Using a Simple Forest Canopy Model", Atmos. Environ. *27A*, p. 1673-1690.

Morris, R.E. and Myers T., 1990, "User's Guide for the Urban Airshed Model - Volume I: User's Guide for UAM(CBIV)", EPA-450/4-90-007a, U.S. Environmental Protection Agency, Research Triangle Park, North Carolina.

Rayner, K.N., Bell, B.P. and Watson, I.D., 1990, "Coastal Internal Boundary Layers and Chimney Plume Dispersion", Proceedings of the International Clean Air Conference, Auckland, March 1990, p. 151-158.

Rye, P.J., 1982, "A Finite-Difference Pollutant Dispersal Model for the Kwinana Region", Technical Report KAMS-22, Department of Environmental Protection, Western Australia.

Rye, P.J., 1989, "Evaluation of a Simple Numerical Model as a Mesoscale Weather Forecasting Tool", *J. Appl. Met.*, **28**, 1257-1270.

Rye, P.J., 1996a, "Meteorological and Source Analysis of Smog Events During the Perth Photochemical Smog Study", Department of Environmental Protection Technical Series 83.

Rye, P.J., 1996b, "Modelling the Meteorology of Perth Photochemical Smog Events", Department of Environmental Protection Technical Series 84.

Scheffe, R.D. and Morris, R.E., 1993, "A Review of the Development and Application of the Urban Airshed Model", *Atmos. Environ.*, **27B**, 23-39.

Stuart, A, and Carnovale, F., 1994, "Perth Photochemical Smog Study Area Based Emissions Inventory", Environmental Protection Authority of Victoria, May 1994.

Zilintinkevitch, S.S., 1972. "On the determination of the height of the Ekman boundary layer", Bound. Layer Met. **3**, 141-145.